AD-A047 239 ROME AIR DEVELOPMENT CENTER GRIFFISS AFB N Y F/G 9/5
TRENDS IN ARRAY ANTENNA RESEARCH,(U)
JUN 77 R J MAILLOUX
UNCLASSIFIED RADC-TR-77-195 NL

| OF |
ADA047 239

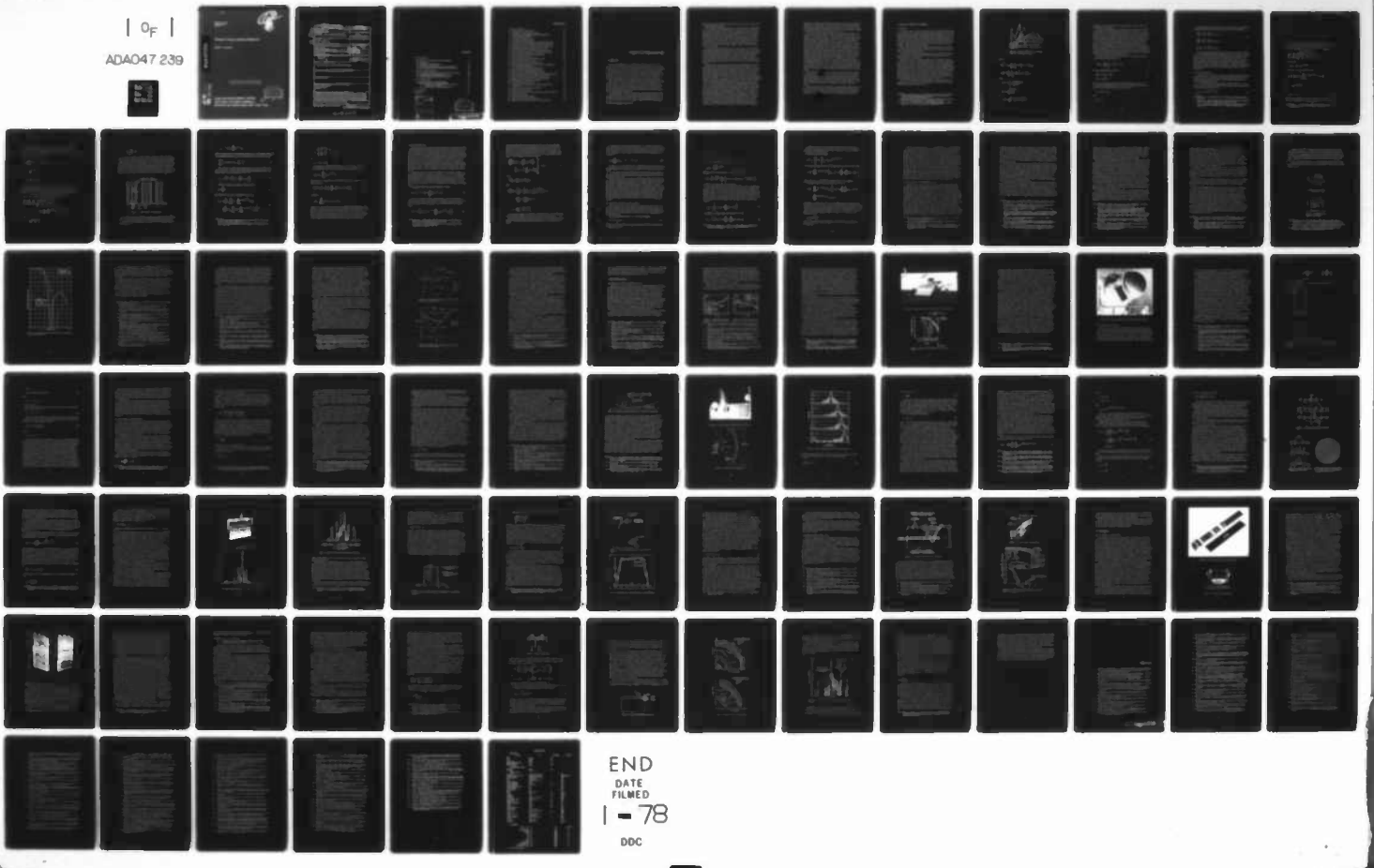

END
DATE FILMED
1-78
DDC

RADC-TR-77-195
IN-HOUSE REPORT
JUNE 1977

Trends in Array Antenna Research

ROBERT J. MAILLOUX

ROME AIR DEVELOPMENT CENTER
AIR FORCE SYSTEMS COMMAND
GRIFFISS AIR FORCE BASE, NEW YORK 13441

Unclassified

SECURITY CLASSIFICATION OF THIS PAGE (When Data Entered)

REPORT DOCUMENTATION PAGE	READ INSTRUCTIONS BEFORE COMPLETING FORM
1. REPORT NUMBER: RADC-TR-77-195 (14)	2. GOVT ACCESSION NO. / 3. RECIPIENT'S CATALOG NUMBER
4. TITLE (and Subtitle): TRENDS IN ARRAY ANTENNA RESEARCH (6)	5. TYPE OF REPORT & PERIOD COVERED: Inhouse
	6. PERFORMING ORG. REPORT NUMBER
7. AUTHOR(s): Robert J. Mailloux (10)	8. CONTRACT OR GRANT NUMBER(s)
9. PERFORMING ORGANIZATION NAME AND ADDRESS: Deputy for Electronic Technology (RADC/ETER) Hanscom AFB Massachusetts 01731	10. PROGRAM ELEMENT, PROJECT, TASK AREA & WORK UNIT NUMBERS: 61102F (16) 23050401 (17) J4
11. CONTROLLING OFFICE NAME AND ADDRESS: Deputy for Electronic Technology (RADC/ETER) Hanscom AFB Massachusetts 01731	12. REPORT DATE: June 1977 (11) / 13. NUMBER OF PAGES
14. MONITORING AGENCY NAME & ADDRESS(if different from Controlling Office): (12) 89 p.	15. SECURITY CLASS. (of this report): Unclassified / 15a. DECLASSIFICATION/DOWNGRADING SCHEDULE

16. DISTRIBUTION STATEMENT (of this Report)

Approved for public release;distribution unlimited.

17. DISTRIBUTION STATEMENT (of the abstract entered in Block 20, if different from Report)

18. SUPPLEMENTARY NOTES

19. KEY WORDS (Continue on reverse side if necessary and identify by block number)

Phased array antennas
Antenna scanning
Antennas

20. ABSTRACT (Continue on reverse side if necessary and identify by block number)

This paper describes a number of analytical developments in the history of phased array research and analyzes the present state of maturity of that field. The main conclusion of this study is that the technology is evolving so rapidly, and the number of different array types and requirements growing so swiftly, that past analytical developments are vastly inadequate to handle the problems posed by present day array systems. The paper highlights those areas where intensified research is necessary.

DD FORM 1 JAN 73 1473 EDITION OF 1 NOV 65 IS OBSOLETE

Unclassified

SECURITY CLASSIFICATION OF THIS PAGE (When Data Entered)

309 050

1B

Contents

Illustrations

Trends in Array Antenna Research

I. INTRODUCTION

The electromagnetic theory of antennas has long been an area of fruitful research with obvious application to the mission-oriented goals of the Air Force. Phased array research is a newer discipline but the emergence of this technology, based upon the apparently simple combination of antenna elements, has been a strong impetus for research on some extremely subtle and intriguing diffraction phenomena. This flurry of activity began in the mid-1960's with the discovery of anomalous scanning behavior in array radiators, and resulted in substantial advances in the theory and measurement of element interaction and its effects.

Most significant is that the stimulus came from a technological advance within a mature field of research, and that these new discoveries required yet more detailed research. At present the study of array phenomena is itself reaching a state of maturity and many of the canonical problems are now understood, but again a vast number of important research areas are being uncovered because of the accelerating pace of innovation.

This paper reflects the thesis stated above, and expresses the belief that the study of phased arrays, far from the stage of merely typing down loose ends, is emerging as an even more fruitful, productive and increasingly relevant area for Air Force sponsored research. The paper is intended to highlight the technical

(Received for publication 15 June 1977)

developments and requirements that provide stimulus, and the most obvious areas requiring intensified research.

Electronically scanned (phased) arrays have found practical use in applications requiring a rapid change in antenna pattern as a function of time, and fixed beam array antennas are used to produce certain specialized beam patterns that cannot be adequately reproduced by lens or reflector geometries. The most important application to date has been to large ground based array radars for surveillance and air traffic control, and this application is primarily responsible for most of the development that has taken place. Other important applications have been to multifunction aircraft arrays and various smaller communications arrays, but progress in these fields is limited by the weight, complexity, and primarily the cost of array systems.

The major factors influencing the future of array antennas are the weight of these past developments, the accelerating pace of technology, cost, and the burden of meeting new requirements imposed by systems that are currently being planned. As noted above, the most important factor to date has been the development of large ground based arrays like the FPS-85, Hapdar, Cobra Dane, and others. These major efforts have stimulated research into array element coupling, space and corporate feeds and microwave circuit components like diode and ferrite phase shifters.

Future trends in array research may not be so closely aligned to the needs of ground based radar, but instead the more fruitful paths will originate from the requirements of a growing list of special purpose arrays; that is, arrays designed for the single application that is their intended use. Many new system specifications require arrays with such unique characteristics that the only economical solution is to design the array tailored to the task at hand. Costs can be reduced by production methods, but in certain cases they are reduced far more dramatically by choice of array type. In addition to cost, new array systems will be required to meet increasinly difficult performance specifications. Most important of these are the low sidelobe characteristics required for defense against antiradiation missiles, and the null steering requirements of broadband antijam communication links. New system types place their own demands upon the antenna circuits, and the growth of satellite communications requirements has become a stimulus for both satellite and aircraft antenna technology. Similarly, the rate of growth of microwave technology itself is a stimulus to array development. Examples will be cited later to show that the fact of an advancing technology with new transmission media and with solid state microwave transmitters or receivers available at each element, has become an increasingly strong driving force for array research. Conventional array elements are not well suited to couple into new stripline and microstrip transmission circuits, and thus a number of different

elements have recently been developed and many more will soon be developed for application to scanning arrays. This fact, coupled with the radiating and reflecting properties of active and adaptive antenna circuits, provide a collection of new and very difficult phased array analysis problems that will challenge the technology and chart the course of research for many years to come.

This survey attempts to deal with these historical forces and influences, that affect the future of array research. Section 2 describes the basic analytical formulation for a typical array problem. The presentation is tutorial in style; scalar equations are used wherever possible in order to avoid the added complexity of vectorial solutions. In general there has been no attempt to survey all of the possible kinds of analytical solution to any one problem; the analysis is included because it aids in explaining some of the physical phenomena observed in phased array systems, and because it serves to illustrate the magnitude of the analytical problem for the case of finite arrays. Section 3 describes several new array geometries categorized as "Special Purpose Arrays"; these are typical responses to specific system problems that require arrays subject to external constraints. The special purpose arrays considered are conformal arrays, arrays for hemispherical coverage and null steering, and array techniques for limited sector coverage and multiple frequency arrays. Section 4 describes certain aspects of new technology that will serve to force the development of arrays with novel kinds of stripline and microstrip elements. Radomes, polarizers and spatial filters are also described in Section 4; these components are undergoing an intense period of change and their design is becoming integral with the associated array or antenna design.

In addition to these areas, there are many other topics that can be expected to affect the future of arrays and array research. Some of these which have not been discussed here are problems associated with antennas over the earth, the science of HF ground screen development, transient analysis of arrays, and the impact and technology of the various active and adaptive array techniques. These were omitted because their proper consideration is beyond the scope of this paper.

These are but a few of the requirements, the technology and the trends. Subject to the author's personal biases and limited perspective, these describe the present state of the technology. Each of the contributing factors is discussed to present a cohesive exposition of this one view of the future of array antennas.

2. THE ARRAY AS A BOUNDARY VALUE PROBLEM

2.1 Introduction

An analytical study of phased array radiation follows the conventional approach from diffraction theory of obtaining solutions of Maxwell's equations for two spatial regions; the external region is free space and the internal region is the inside of the various transmission lines or waveguide exciting the radiating elements. The solution in the exterior region must satisfy the boundary conditions that apply on the surface supporting the array, and this gives rise to the major problems in the analysis of arrays conformal to specific structures like aircraft or spacecraft antennas, or arrays mounted over the earth.

Most often the exterior region is considered to be unbounded or bounded by a half space; in these circumstances the Greens function is derived from combinations of retarded potential type terms.

The dyadic form of Green's symmetrical theorem gives the free space fields in terms of integrals over all currents, charges, and aperture fields in the exterior space or on its boundary.[1]

Although arrays are as commonly comprised of wire elements as aperture elements, this review will treat only the aperture case. The dual situation involving wire elements leads to field expressions derivable from vector potential integrals over the currents in the wires and their images, and the resulting boundary value problem arising at the array face is a series of integral equations on the surfaces of the wires. In these cases, the interior field solution is usually idealized to the extent that the fields are replaced by a delta function voltage source as in Hallen's[2] equation. More recent work has removed some of these assumptions about the idealized nature of the source and has considered the implications of the use of an approximate kernal for the Greens function for wires.[3]

The free space field in the half space bounded by a perfectly conducting half plane with an array of apertures as shown in Figure 1 can be written in terms of integrals over the aperture fields as shown.[1]

---

1. Levine, H., and Schwinger, J. (1950, 1951) On the theory of electromagnetic wave diffraction by an aperture in an infinite plane conducting screen, Comm. on Pure and Applied Math 44:355-391.
2. Hallen, Erik (1938) Theoretical investigations into transmitting and receiving antennae, Nova Acta Regiae Soc. Sci. Upsaliensis (4) 11(No. 1).
3. King, R. W. P., and Harrison, C. W. (1969) Antennas and Waves, a Modern Approach, MIT Press, Cambridge, MA, (See Section 3.10).

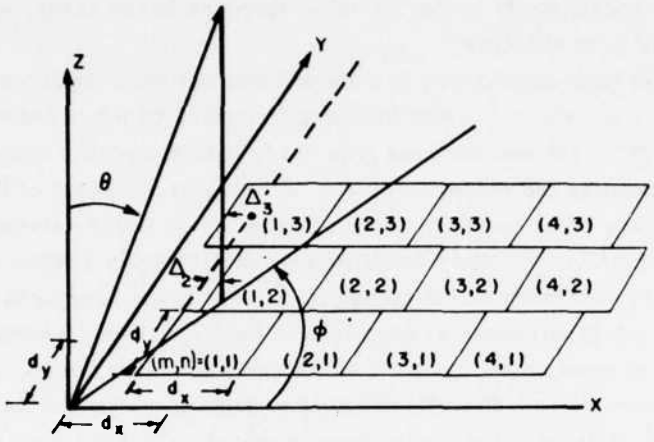

Figure 1. Array Coordinates. Element center locations $x = md_x + \Delta_{n'}$, $y = nd_y$

For $z \geq 0$

$$\bar{B}(\bar{r}) = j2\omega\mu\epsilon \sum_m \int_{S_m} \underline{\Gamma}^o(\bar{r}, \bar{r}') \cdot (\hat{z} \times \bar{E})\, dS'_m$$

$$\bar{E}(\bar{r}) = 2 \sum_m \int_{S_m} \overline{\nabla G}(\bar{r}, \bar{r}') \times (\hat{z} \times E)\, dS'_m \qquad (1)$$

where

$$\underline{\Gamma}^o(r, r') = \left(\underline{U} + \frac{1}{k_o^2}\underline{\nabla\nabla}\right) G(\bar{r}, \bar{r}') \qquad (2)$$

and

$$G(r, r') = \frac{e^{-jk_o|\bar{r}-\bar{r}'|}}{4\pi|\bar{r} - \bar{r}'|}$$

and

$$|\bar{r} - \bar{r}'| = \sqrt{(x - x')^2 + (y - y')^2 + z^2} \quad .$$

The index "m" corresponds to the "m' th" – aperture in the array, and $\hat{z} \times E$ is evaluated at the m'th aperture.

An $\exp(+j\omega t)$ time dependence is assumed and has been suppressed. Vectors are denoted by a far above the expression and dyadics by a bar below. $\underline{U}$ is the unity dyad and $\underline{\Gamma}^o$ is the conventional free space dyadic Green's function. Equation (2) is used to express the radiation fields, and also as the basis of the electromagnetic boundary value problem at the junction of the fields determined from (2) satisfy the appropriate boundary conditions on the perfectly conducting plane at $Z = 0$ and assure continuity of the tangential $\overline{E}$ field at the apertures. One can obtain a set of integrodifferential equations at each aperture by expanding the fields in the feed waveguides in terms of TE and TM modes, using the internal $\overline{E}$ field as the tangential $(\hat{z} \times \overline{E})$ aperture field in each aperture and then equating the magnetic fields of the internal and external expansions across each aperture. This procedure is extremely cumbersome and has not been carried out in such generality except for several distinct canonical geometries.

An expression which is entirely equivalent to (2) is obtained by defining the magnetic Hertzian potential $\overline{\Pi}_m(\overline{r})$ as:

$$\overline{\Pi}_m(\overline{r}) = j2 \sum_m \int_{S_m} (\hat{z} \times \overline{E})\, G(r, r')\, dS'_m \quad . \tag{3}$$

The corresponding fields are written

$$\overline{B}(\overline{r}) = \nabla(\nabla \cdot \overline{\Pi}_m) + k_o^2 \overline{\Pi}_m \tag{4}$$

$$\overline{E}(\overline{r}) = -j\omega \nabla \times \overline{\Pi}_m \quad .$$

For the case of rectangular waveguides exciting rectangular apertures, one can expand the waveguide fields in terms of magnetic potential functions by defining two scaler Hertzian potentials Π'_{mx} and Π'_{my} such that:

$$\overline{\Pi}'_m = \hat{x}\Pi'_{mx} + \hat{y}\Pi'_{my} \tag{5}$$

and

$$\Pi'_{mz} = 0 \quad .$$

Equating tangential fields in the apertures leads to the following equations for the difference between internal and external Hertzian potential components.

$$\left(\frac{\partial^2}{\partial x^2} + \frac{\partial^2}{\partial y^2} + k_o^2\right)(\Pi'_{mx} - \Pi_{mx}) = 0$$

$$\left(\frac{\partial^2}{\partial x^2} + \frac{\partial^2}{\partial y^2} + k_o^2\right)(\Pi'_{my} - \Pi_{my}) = 0 \qquad (6)$$

$$\frac{\partial}{\partial x}(\Pi'_{mx} - \Pi_{my}) = \frac{\partial}{\partial y}(\Pi'_{mx} - \Pi_{mx}) \qquad (7)$$

These three integrodifferential equations, repeated at each aperture, define all of the radiation and interelement coupling for the array of aperture. They are similar to those obtained for a number of classical diffraction problems,[4] and clearly show the vector nature of the solution unless $\partial/\partial x$ or $\partial/\partial y$ are zero. Arrays scanned in a single plane and with translational invarience in the second plane can have scalar field solutions. In addition, it is often convenient and appropriate to neglect the crosspolarized component of radiation or coupling when that neglect can be shown to have no adverse effect upon the critical aspects of the solution.[5, 6]

2.2 Solution for an Infinite Array

The kernal of Eq. (3) involves a summation of retarded field integrals over the elements of an array. The special case of an equally spaced infinite array provides particularly simple form of kernal that has solutions with the form of Floquet's spatial harmonic series.

For a two-dimensional array with dimensions shown in Figure 1, the main beam of the array is scanned to an angle (θ_o, ϕ_o) by application of incident fields in each waveguide (p, q) having the form:

$$E_{inc} = E_o\, e^{-jk_o(u_o m d_x + v_o n d_y)} \qquad (8)$$

---

4. Bouwkamp, C.J. (1954) Diffraction theory, Reports on Progress in Physics 17:35-100.
5. Mailloux, R.J. (1969) Radiation and near-field coupling between two collinear open-ended waveguides, IEEE Trans. AP-17(No. 1):49-55.
6. Lewin, L. (1970) On the inadequacy of discrete mode-matching techniques in some waveguide discontinuity problems, IEEE Trans. MTT-18(No. 7): 364-372.

where

$$u_o = \sin\theta_o \cos\phi_o$$

$$v_o = \sin\theta_o \sin\phi_o \tag{9}$$

$$k_o = 2\pi/\lambda_o$$

and (u_o, v_o) are the direction cosines of the main beam position vector.

This periodic incident field results in the same periodicity in the aperture field and the accompanying simplification of the summations.

For the case of an array scanned in one plane, summations of the form

$$\int_{x'}\int_{y'} \sum_{m=-\infty}^{\infty} \frac{e^{-jk_o\sqrt{(x-x'_m)^2+(y-y')^2+z^2}}}{\sqrt{(x-x'_m)^2+(y-y')^2+z^2}} E(x'_m, y') \tag{10}$$

become, using

$$E(x_m, y) = E(x_o, y)\, e^{-jk_o u_o m d_x}$$

and using $x'_m = x'_o + md_x$, the above yields:

$$\int_{x'}\int_{y'} \frac{-j\pi}{d_x} (E(x'_o, y') \sum_{m=-\infty}^{\infty} e^{-jk_o u_m (x-x'_o)(2)} H_o\left(k_o r\sqrt{1-u_m^2}\right) \tag{11}$$

where

$$r = \sqrt{(y-y')^2 + z^2}$$

and

$$u_m = u_o + m/d_x$$

This form shows that the series is now summed over the spatial parameter u_m and has the characteristics of a spatial harmonic[7] series in this parameter. To

7. Brouillion, L. (1953) Wave Propagation in Periodic Structures, Dover Publications, Inc.

complete the evaluation of Eq. (3), this equation must be integrated over the y' parameter, and the near fields thus assume a relatively complex form in general. In the special case of infinite slots in the y' dimension with $\partial y = 0$ the series takes on an extremely simple form even in the near field. After performing this integration, expression 11 becomes:

$$\frac{j2\pi}{d_x} \sum_{m=-\infty}^{\infty} \frac{e^{-j(K_m|z| + k_o u_m x)}}{K_m} F(u_m) \tag{12}$$

where

$$K_m = k_o \sqrt{1 - u_m^2}$$

and

$$F(u_m) = \int_{x'} E(x')\, e^{jk_o u_m x'}\, dx' \quad .$$

This expression is now clearly the sum over a series of waves that propagate or decay outside of the array depending upon whether K_m is real or imaginary. The sum is called a grating lobe series and the spatial angles at which $\exp[K_m|z| + k_o u_m x]$ is unity are grating lobe angles. The field in space is thus represented as an infinite series of waves with excitation coefficients $F(u_m)$.

For an array scanned in both planes, the summations become:

$$\int_{x'} \int_{y'} \sum_{n=-\infty}^{\infty} \sum_{m=-\infty}^{\infty} \frac{e^{-jk_o \sqrt{(x-x'_m)^2 + (y-y'_n)^2 + z^2}}}{\sqrt{(x - x'_m)^2 + (y - y'_n)^2 + z^2}} \tag{13}$$

$$= -\frac{1}{d_x d_y} \sum_m \sum_n \frac{e^{-j(k_o u_m + k_o v_n + K_{mn})}}{K_{mn}} F(u, v)$$

where here

$$K_{mn} = k_o \sqrt{1 - u_m^2 - v_n^2}$$

and

$$F(u, v) = \int_{y'} \int_{x'} E(x', y')\, e^{jk_o(ux'+vy')}$$

For an array scanned in one plane and under certain special circumstances, the array electromagnetic field can be scalar. Examples of such scalar problems are the E-plane scan of a parallel plane array with TEM incident modes, and H-plane scan of the array shown in Figure 2. This array geometry is a novel design and uses the properties of dielectric slab loaded waveguides to support efficient radiation at two frequencies that are separated by about an octave. Since $\partial y = 0$ the array is equivalent to a parallel plane structure for H-plane scan. This equivalence is shown by removal of the horizontal metal separators at $y = \frac{dy}{2}(2n - 1)$.

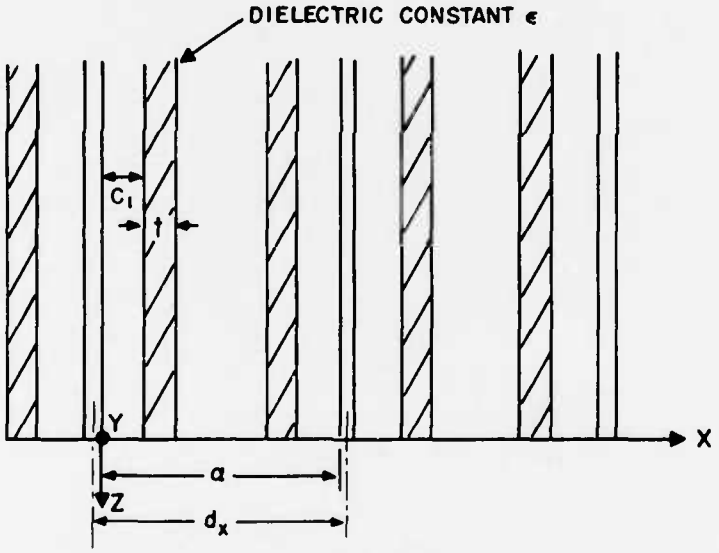

Figure 2. Array Geometry – H-Plane Scan

The solution proceeds by expanding the waveguide fields in terms of an infinite series of waveguide modes ($LSE_{p,o}$) and using this field expansion in Eq. (6).

The interior potential function for a mode with transverse incident field distribution $e_p(x)$ is:

$$\Pi_p = e^{-\gamma_p z} e_p(x) - \sum_{q=1}^{\infty} \Gamma_q e^{\gamma_q z} e_q(x) \tag{14}$$

where γ_p and γ_q are the modal propagation constants for the slab loaded waveguide.[8] The waveguide eigenfunctions $e_p(x)$ are orthogonal[9] and are normalized so that

$$\int_{-a/2}^{a/2} e_p(x)\, e_q(x)\, dx = \delta_{pq} = \begin{cases} 1 & p = q \\ 0 & p \neq q \end{cases} . \tag{15}$$

The coefficients Γ_q give the amplitude and phase of the waves reflected from the aperture face ($z = 0$) and include propagating and nonpropagating modes. The aperture field for the incident mode P is (at $z = 0$)

$$E_{y_p} = -j\omega \frac{\partial \Pi_p}{\partial z} = j\omega \left[\gamma_p e_p(x) + \sum_{q=1}^{\infty} \Gamma_q \gamma_q e_q(x) \right] . \tag{16}$$

Within the waveguides the magnetic field is given by

$$B = -\frac{\partial^2 \Pi}{\partial x^2} \tag{17}$$

and in the exterior region it is obtained from Eq. (4) as:

$$B_{x_p} = -\frac{1}{d_x} \left[\gamma_p \int_{-a/2}^{a/2} e_p(x') \sum_{m=-\infty}^{\infty} e^{-j\beta_m (x-x')} \xi_m \, dx' \right.$$
$$\left. + \sum_{q=1}^{\infty} \Gamma_q \gamma_q \int_{-a/2}^{a/2} e_q(x') \sum_{m=-\infty}^{\infty} e^{-j\beta_m (x-x')} \xi_m \, dx' \right] \tag{18}$$

8. Seckelmann, R. (1966) Propagation of TE modes in dielectric loaded waveguides, IEEE Trans. MTT-14:518-527.

9. Collin, R.E. (1960) Field Theory of Guided Waves, McGraw-Hill Book Co., Inc., New York.

where

$$\xi_m = \begin{cases} j\sqrt{k_o^2 - \beta_m^2} & \text{for} \quad \beta_m^2 > k_o^2 \\ \sqrt{\beta_m^2 - k_o^2} & \text{for} \quad \beta_m^2 < k_o^2 \end{cases}$$

and

$$\beta_m = k_o [u_o + m/d_x] \quad .$$

Equating these magnetic field expressions at z = 0, truncating the series at q = Q, multiplying by $e_\ell(x')$, using orthogonality and defining the integral

$$\text{Int}_q(\beta_m) = \int_{-a/2}^{a/2} e_q(x')\, e^{+j\beta_m x'}\, dx' \tag{19}$$

one obtains a set of Q equations for the Q coefficients at Γ_q for the incident p'th mode excitation:

$$\left[\delta_{p\ell}\, \gamma_p^2 - \frac{1}{d_x}\gamma_p\, \mathscr{A}_{p\ell}\right] = \sum_{q=1}^{Q} \Gamma_q \left[\gamma_q^2 \delta_{q\ell} + \frac{1}{d_x}\gamma_q\, \mathscr{A}_{q\ell}\right] \qquad \text{for} \quad \ell = 1 \text{ to } Q \tag{20}$$

and where

$$\mathscr{A}_{q\ell} = \sum_{m=-M}^{M} \xi_m\, \text{Int}_q(-\beta_m)\, \text{Int}_\ell(\beta_m) \quad .$$

Solution of the above matrix equation gives the waveguide field distribution at each aperture, and includes all of the mutual coupling effects for the infinite array. The particular array studied here uses two incident modes (p = 1, 2) at the high frequency, and so the set of equations above must be solved twice to obtain a solution for the combined two mode excitation. The series over m is truncated at ±M (usually between 40 and several hundred terms) as required for convergence.

2.3 Analysis for a Finite Array

Solutions like the above have been extremely useful for the analysis and design of large arrays such as those used for ground based radar. Smaller arrays with ten or fewer elements in each plane have behavior dominated by edge effects and for these the infinite array analysis has little meaning. There have been analytical treatments[10, 11] of semiinfinite arrays that give insight into the phenomena of edge effects in large arrays without including higher order modal effects. The vast majority of finite array studies have been performed using a scattering matrix that includes only a single waveguide mode; a procedure that can be highly inaccurate when the array is operated at a frequency or scan angle near which an array resonance can occur. These resonances or "blind-spots" have been the subject of substantial controversy over the past decade and will be described in more detail later.

Equation (20) can be rewritten as an infinite set of simultaneous equations and then truncated to yield a solution of any desired accuracy. This is accomplished by expanding the field in each mth waveguide in terms of a sum over all incident and reflected modes. In general this involves both components of the vector solution, but again it is more convenient for the purposes of illustrations to restrict the analysis to a finite array of "M" of the infinite columns of Figure 2 for H-plane scan.

The potential function for the mth waveguide is written:

$$\Pi(m) = a_m e^{-\gamma_1 z} e_1(x') - \sum_{q=1}^{\infty} b_m^q e^{-\gamma_q z} e_q(x') \quad . \tag{21}$$

Here it is assumed that only the single dominant mode is incident in each waveguide, but that all modes are reflected. The notation b_m^q is the coefficient of the q'th reflected mode in waveguide m. After obtaining the aperture electric field

$$E(m) = j\omega \left[a_m \gamma_1 e_1(x') e^{-\gamma_1 z} + \sum_{q=1}^{\infty} b_m^q \gamma_q e^{-\gamma_q z} e_q(x') \right] \tag{22}$$

10. Borgiotti, G. V. (1971) Edge effects in finite arrays of uniform slits on a groundplane, IEEE Trans. AP-19(No. 5):593-599.

11. Wasylkiwskyj, W. (1973) Mutual coupling effects in semi-infinite arrays, IEEE Trans. AP-21(No. 3):277-285.

and inserting this field in the integrodifferential Eq. (6) or into the equivalent equation obtained by equating the tangential magnetic fields at both sides of the aperture as in Eq. (20). The resulting equation, multiplied by the sequence of $e_1(x)$ for $\ell = 1$ to Q and integrated over x yields a series of "Q" algebraic equations at each aperture and can be written in the form of a nultimodal scattering matrix. The l'th equation at the mth waveguide is:

$$\left.\begin{aligned} \sum_{q=1}^{Q}\left[b_m^q \gamma_q^2 \delta_{q,\ell} - \sum_{n=1}^{N} b_n^q \gamma_q \mathcal{Q}_{mn}^{q\ell}\right] \\ = \left[a_m \delta_{q,\ell} \gamma_1^2 + \sum_{n=1}^{N} a_n \gamma_1 \mathcal{Q}_{mn}^{1\ell}\right] \end{aligned}\right\} \quad \ell = 1, Q \qquad (23)$$

where

$$\mathcal{Q}_{mn}^{q\ell} = \frac{1}{2\Pi} \int dx\, e_\ell(x)\, \mathcal{K}_{mn}^{q\ell}(x)$$

and

$$\mathcal{K}_{mn}^{q\ell}(x) = \left(\frac{\partial^2}{\partial x^2} + k_o^2\right) \int_{x'} e_q(x') \int_{-\infty}^{\infty} \frac{e^{-jk_o|r-r'|}}{|r - r'|} dx'\, dy'$$

$$= \left(\frac{\partial^2}{\partial x^2} + k_o^2\right) \int_{x'} e_q(x')\, dx'$$

for

$$|r - r'| = \sqrt{(x_m - x_n')^2 + (y')^2} \quad .$$

N such sets of equations are required, one set at each aperture, thus leading to a set of N × Q equations to be solved to complete the array solution.

The numerical evaluation of solutions like the one above are indeed formidable, and the solution is most often approximated using only one or two terms of the series.

Although the most common analytical practice is to assume a set of incident fields {a} and solve the set (23) for the reflected signals $\{b\}^q$ for all modes q, one could obviously assume a sequence of independent incident modes and solve the set for each incident a_m. This solution is the scattering matrix for each mode q of the array.

$$b_m^q = \sum_{n=1}^{N} S_{mn}^q a_n \qquad \text{or} \qquad b^q = S^q a \quad . \tag{24}$$

Written in this form there are Q such scattering matrices required to describe the Q waveguide modes reflected from the apertures (for a single mode incident on each).

It is important to observe that the whole set of higher order modes enters into the Eq. (24), and so the scattering coefficients S_{mn}^q include the mutual coupling of these higher order modes.

Arrays with more than one incident mode (like that of Figure 2) can be analyzed by repeating the above procedure for the several incident modes and superimposing the solutions. Although this formulation gives a complete solution of the multi-element array radiation and interelement problem, the amount and complexity of the required numerical analysis often makes such a solution impractical. Suitable approximations include using only one or several modes in each waveguide, neglecting cross-polarized interactions, utilizing asymptotic approximations of the scattering coefficients for the widely spaced elements and neglecting the interaction between the higher order modes in the evaluation of scattering coefficients. The implications of several of these approximations will be discussed in subsequent sections.

2.4 Array Radiation and the Concept of an Element Pattern

Equation (4) gives the complete radiated field for an array of apertures in a perfectly conducting plane. Determination of the tangential E fields in these apertures is achieved by solving the boundary value problem at the waveguide/aperture interface by the methods outlined in a previous section, or by other techniques to be mentioned later.

The far field approximation to Eq. (2) is obtained by using

$$|\bar{r} - \bar{r}'| \doteq R_o - \bar{r}' \cdot \hat{\rho} \tag{25}$$

where R_o is measured from the coordinate origin in the aperture to the given point in space at R_o, θ, ϕ and

$$\overline{r}' = \hat{x}\, x' + \hat{y}\, y'$$

and

$$\hat{\rho} = \hat{x}\, u + \hat{y}\, v + \hat{z} \cos\theta \quad . \tag{26}$$

Using this approximation, it is customary to write

$$G(\overline{r}, \overline{r}') = \frac{e^{-jk_o R_o}}{4\pi R_o} e^{jk_o(\overline{r}' \cdot \hat{\rho})} \quad .$$

Evaluation of Eq. (2) for apertures in the plane z = 0 yields:

$$E(\overline{r}) = \frac{jk_o}{2\pi} \frac{e^{-jk_o R_o}}{R_o} \sum_m \int_{S_m} dS_m \left[\cos\theta\, \overline{E}_T(x'_m, y'_m) - \hat{z}\hat{\rho} \cdot \overline{E}_T(x'_m, y'_m)\right]$$

where $\overline{E}_T$ is the tangential field in the aperture.

This relationship is also given in the text by Amitay et al.[12] The tangential field $\overline{E}_T$ is a two component vector in general, but for the array of Figure 2 and (approximately) for the case of thin slots, the aperture field can be described by a single component. For tutorial purposes the remainder of this description will treat the scalar case in which the cross-polarized radiation is neglected or identically zero and the waveguide polarization is in the y direction. In this case, the aperture fields are written using Eq. (4). The field in the m'th waveguide (at z = 0) is:

$$E_{y_m} = j\omega \left[a_m \gamma_1 e_1(x') + \sum_{q=1}^{Q} b_m^q \gamma_q e_q(x') \right] \tag{27}$$

or, using the scattering matrix representation of Eq. (24)

$$E_{y_m} = j\omega \left[a_m \gamma_1 e_1(x') + \sum_{n=1}^{M} a_n \sum_{q=1}^{Q} e_q(x')\, S_{mn}^q\, \gamma_q \right] \quad . \tag{28}$$

12. Amitay, N., Galindo, V., and Wu, C. P. (1972) Theory and Analysis of Phased Array Antennas, New York, Wiley Interscience.

Unlike the infinite array, Eq. (28) shows that a finite array with periodic incident fields has nonperiodic aperture fields because of the lack of symmetry in the element scattering matrices.

Defining the aperture integrals

$$I_q(u, v) = \int_{-a/2}^{a/2} dx' \int_{-b/2}^{b/2} dy'\, e_q(x', y')\, e^{jk_o(x'u+y'v)} \tag{29}$$

one obtains (neglecting constants) the following expression for the array far field

$$F(\theta, \phi) = \sum_{m=1}^{M} e^{+jk_o(ux_m+vy_m)} \left\{ a_m \gamma_1 I_1(u, v) + \sum_{n=1}^{M} a_n \sum_{q=1}^{Q} S_{mn}^{q} \gamma_q I_q(u, v) \right\} \tag{30}$$

where x_m and y_m are the position coordinates for the m'th waveguide.

This expression can be rewritten in the following form:

$$F(\theta, \phi) = \sum_{m=1}^{M} e^{jk_o(ux_m+vy_m)}\, j\omega a_m \left[\gamma_1 I_1(u, v) + \sum_{n=1}^{M} \sum_{q=1}^{Q} S_{mn} \gamma_q I_q(u, v) \right] \tag{31}$$

$$= \sum_{m=1}^{M} e^{jk_o(ux_m+vy_m)}\, a_m f_m(\theta, \phi)$$

which makes it evident that the far-field is a superposition of fields due to each element located at position x_m, y_m, excited by a coefficient a_m and having a spatial variation $f_m(\theta, \phi)$. For a large planar array forming a single pencil beam, one can show that the main beam gain is related to the square of the magnitude of this sum times cos θ except for angles very near to end-fire. Thus, for a large, two-dimensional array

$$f_m(\theta, \phi) \sqrt{\cos \theta}$$

is the element pattern of the m'th element. The cos θ term is not present for a column array.

Like the aperture distribution, this element pattern differs for each element of a finite array. Furthermore, the element pattern has in it all of the effects of mutual coupling and so can be an extremely complex function of the space coordinates (θ, ϕ). Proper element pattern control is the prime requisite of array design, and the formidable task of element pattern evaluation is not a choice to be taken lightly. Unfortunately, the history of phased array development reveals the closeted skeletons of arrays that were built using single mode approximations for mutual coupling. These and other details will be described in subsequent sections, but it is important to note here that the pattern $f_m \sqrt{\cos \theta}$ of the m'th element is exactly what one measures in the far field when only that element is excited. Because of reciprocity it is also the signal received at that element from a distant transmitter, and so its measured value includes, for any given array, all of the coupling and higher order modal effects that will be observable when the array is excited as a whole. Element pattern measurement is thus an extremely powerful tool of array design, because it is possible to record this single mode parameter and still account for all of the subtleties that occur at the array face.

2.5 Historical Perspective and the Blindness Phenomena

The previous sections have shown one method of analyzing waveguide arrays including the mutual coupling between all array elements. Waveguide elements were chosen for these examples because they have been the subject of extensive research over the past ten years and because they conveniently illustrate many of the phenomena that will be described later. Early studies of mutual coupling were performed mainly for arrays of dipole elements[13] with assumed sinusoidal current distributions, and later[14, 15] for current distributions that contained several higher order terms to approximate the exact distribution. These analyses were based upon various forms of Hallen's integral equation and the discovery that higher order modes were important came about mainly through the diligence of researchers working in the field. These theoretical efforts were accompanied by extensive experimental programs, and the use of higher order current approximations was motivated primarily by a concern that any analytical solution for current and charge distributions be adequate to allow an accurate description of the near-field. Despite the fact that these earlier dipole array studies were performed many years ago,

13. Carter, P. S., Jr. (1960) Mutual impedance effects in large beam scanning arrays, IRE Trans. AP-8:276-285.

14. King, R. W. P. (1956) The Theory of Linear Antennas, Harvard University Press, Cambridge, MA.

15. King, R. W. P., and Sandler, S. S. (1964) The theory of broadside arrays, and the theory of endfire arrays, IEEE Trans on Antennas and Propagation AP-12:269-275, 276-280.

the dipole has remained a subject of continued interest. Recent analytical studies have been based primarily on moment-method approaches[16, 17] which are applicable to a wide variety of wire antenna shapes and orientations, and for which there are now a number of available computer programs of very great generality. Air Force sponsorship in this area has been a factor of major importance. Starting with the basic studies of Carter[13] and King[14, 15] and continuing to the present day, the Air Force 6.1 effort has funded many of the major analytical developments in dipole antenna arrays.

The recent concern with waveguide arrays reflects the fact that by the mid-1950's the analytical background for this technology lagged far behind that of dipole arrays. Customary waveguide array solutions dealt almost exclusively with single mode approximations to the waveguide field, but did properly account for the full spatial harmonic series (grating lobe series) in the free space half space. Some earlier studies of single radiating waveguides used stationary solutions of the aperture integral equation in order to obtain variational formulas for input impedance,[18, 19] but until the mid-60's there were no published multimodel solutions of even this basic radiating geometry.

If little effort had been devoted to the single radiator problem, even less has been done to describe the coupling between waveguides. One of the first studies of this sort was performed by Wheeler[20] who assumed the coupled radiators were in the far-field of one another. In 1956, Levis[21] derived general equations for a variational formulation to obtain the coupling between a number of generally cylindrical waveguides radiating through a common ground plane. He applied the method to a set of coupled annular slots. Galejs[22] applied a stationary formulation due to

---

16. Harrington, R.F. (1968) Field Computation by Moment Methods, McMillan Co., New York.

17. Harrington, R.F., and Mautz, J.R. (1967) Straight wires with arbitrary excitation and loading, IEEE Trans. AP-15(No.4):502-515.

18. Lewin, L. (1951) Advanced Theory of Waveguides, Iliffe and Sons, Ltd., London, Chapter 6.

19. Cohen, M.H., Crowley, T.H., and Levis, C.A. (1951) The Aperture Admittance of a Rectangular Waveguide Radiating into a Half Space, (ATI-133707) Antenna Laboratory, Ohio State University, Research Foundation, Rept. 339-22.

20. Wheeler, G.W. (1950) Coupled Slot Antennas, Ph.D. Thesis, Harvard University, Cambridge, MA.

21. Levis, C.A. (1956) Variational Calculations of the Impedance Parameters of Couplied Antennas, Ohio State University Research Foundation, Rept. 667-16, Contract AF33(616)3353.

22. Galejs, J. (1965) Self and mutual admittances of waveguides radiating into plasma layers, Radio Sci. J. Res. NBS/USNC-URSI 69D(No.2):179-189.

Richmond[23] to solve the problem of two parallel slots in a ground plane, with both slots backed by waveguides. His method yielded usable and convenient formulas; however, it includes the implicit assumption that the tangential magnetic field at the coupled waveguide aperture is the same as the magnetic field which would be present on the ground plane if the coupled aperture were not present. In this manner, Galejs avoided the problem of solving an integral equation.

Other researches that evolved from the point of view of antenna element coupling were the study by Lyon et al, [24] to determine the power coupling between various structures including arbitrarily oriented open ended waveguide and two studies by Mailloux[25, 26] that dealt with the multiple mode solution of collinear radiating waveguides, and the induction of cross-polarized fields in mutually coupled waveguides with arbitrary orientation. This last paper described some approximate procedures to account for coupling in large arrays where the numerical evaluation of all the higher order terms would otherwise become unwieldy. The use of such interelement coupling approaches to array theory has not been popular until recently, [27, 28] because the coupling integrals are two dimensional with singular kernals and the resulting matrices are often so large that it seemed unreasonable to consider including higher order effects unless there was an extremely good reason to do so. In recent years, this approach has gained some favor because of the availability of large computers and because of an increased awareness of the need for accurate array calculations.

The stimulus that intensified research into array mutual coupling phenomena was called array "blindness," and went undiscovered by university or government sponsored research programs. Its discovery occurred when several array systems exhibited poor scanning performance and so to these investigators "array blindness" was not an interesting phenomenon but a plague; once uncovered, it was

---

23. Richmond, J.H. (1961) A reaction theorem and its applications to antenna impedance calculations, IRE Trans AP AP-8:515-520.

24. Lyon, J.A.M., Kalafus, R.M., Kwon, Y.K., Diegenis, C.J., Ibrahim, M.A.H., and Chen, C.C. (1966) Derivation of Aerospace Antenna Coupling – Factor Interference Predication Techniques, Tech. Rept. AFAL-TR-66-57, The University of Michigan, Radiation Laboratory.

25. Mailloux, R.J. (1969) Radiation and near-field coupling between two collinear open-ended waveguides, IEEE Trans on Antennas and Propagation AP-17: (No. 1):49-55.

26. Mailloux, R.J. (1969) First-order solutions for mutual coupling between waveguides which propagate two orthogonal modes, IEEE Trans. AP-17: 740-746.

27. Bailey, M.C. (1974) Finite planar array of circular waveguide apertures in flat conductor, IEEE Trans. AP-22:178-184.

28. Steyskal, H. (1974) Mutual coupling analysis of a finite planar waveguide array, IEEE Trans. AP-22:594-597.

found in numerous systems and proposed systems. Blindness is evidenced by a null well within the normal scan sector of an array. It is mainly a problem for large arrays and so was not found in tests of arrays that consisted of only a few elements in each plane. Before describing and commenting further on the history of this important development, I would stress that this was an area that should have been uncovered by researchers before it became a crisis to be discovered by system manufacturers. Given the cost and importance of such systems, there was clearly not an adequate concern for fundamental studies at a time when they could have averted the serious problems that followed.

The phenomenon of array blindness became a factor of extreme confusion for a number of years. Examples of this confusion abound throughout the early literature where, for example, one author stresses the importance of including waveguide higher-order modes in any analysis for predicting array blind spots, and another author uses a single-mode theory for a different structure to accurately predict an occurrence.

The reasons for this confusion, as explained by Knittel et al,[29] is that, depending upon the array structure, there are two basic types of cancellation resonances: those that occur external to, and those that occur within the array waveguide apertures.

The waveguide higher-order modes play a dominant role for the internal-type resonance, but are relatively unimportant for an external resonance. This is because the external resonance occurs only for arrays that have a structure of some kind beyond the array face, and the resonance is caused by the interaction between the radiating mode and a higher-order external mode supported by this structure. An internal resonance can be viewed as a cancellation effect between the dominant and a higher-order waveguide mode radiation. An awareness of this distinction is useful for categorizing the various reports of array blind spots.

The first convincing demonstration of the existence of an array null was obtained experimentally by Lechtreck[30] using an array of circularly polarized coaxial horns with separate hemispherically shaped radomes for each element. The null occurred for the electric field perpendicular to the ground plane, and was called an external resonance by Oliner.[31]

---

29. Knittel, G. H., Hessel, A., and Oliner, A.A. (1968) Element pattern nulls in phased arrays and their relation to guided waves, Proc. IEEE 56:1822-1836.

30. Lechtreck, L.W. (1965) Cumulative coupling in antenna arrays, IEEE G-AP International Symposium Digest, 144-149.

31. Oliner, A.A., and Malech, R.G. (1966) Speculation on the role of surface waves, Microwave Scanning Antennas, Academic Press, N.Y., Vol. 2, 308-322.

Farrell and Kuhn[32, 33] presented the first thecretical evidence of internal resonance nulls in all planes of a triangular grid array (Figures 3 and 4) and in the E-plane of a rectangular grid array. They also presented experimental verification of the E-plane rectangular grid null, but they were able to verify the existence of nulls only in the H-plane and intercardinal planes of the triangular grid array.

Amitay and Galindo[34] analyzed circular waveguide phased arrays in rectangular grid orientations and observed that incomplete nulls occur for intercardinal planes of scan.

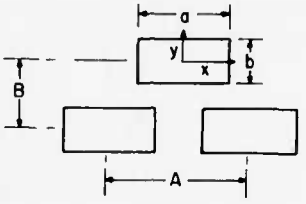

A. TRIANGULAR GRID ARRAY

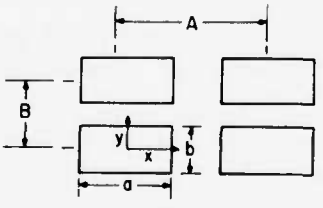

B. RECTANGULAR GRID ARRAY

Figure 3. Triangular and Rectangular Grid Lattices

32. Farrell, G. F., Jr., and Kuhn, D. H. (1966) Mutual coupling effects of triangular-grid arrays by modal analysis, IEEE Trans. AP-14:652-654.

33. Farrell, G. F., Jr., and Kuhn, D. H. (1968) Mutual coupling in infinite planar arrays of rectangular waveguide horns, IEEE Trans. AP-16:405-414.

34. Amitay, N., and Galindo, V. (1968) The analysis of circular waveguide phased arrays, Bell System Technical Journal, 1903-1932.

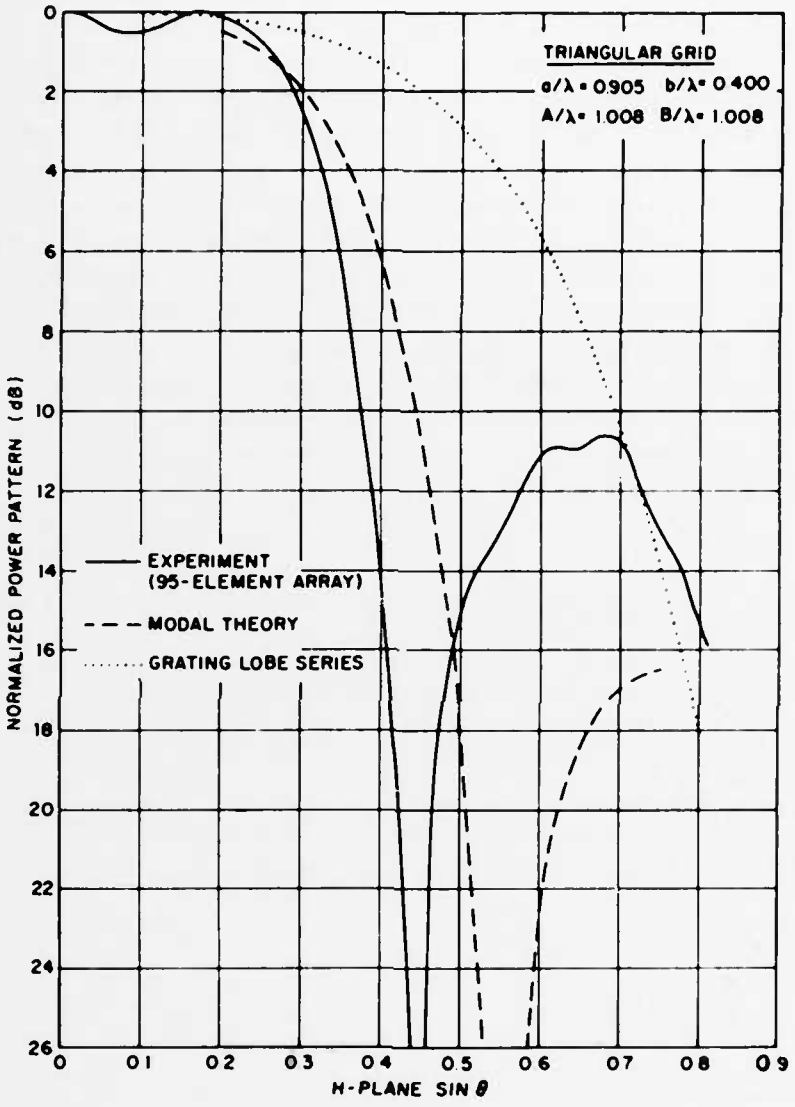

Figure 4. Array Element Power Pattern Showing Array Blindness (From Farrel and Kuhn[33])

DuFort[35, 36] found nulls for a TE mode parallel plate array and a triangular grid array of rectangular waveguides on an H-plane corrugated surface, and Mailloux[37] found blind spots for the E-plane scan of an array of TEM mode parallel plane waveguides with conducting fences between adjacent radiators. To the extent that these effects occur because of the external structure, they are external resonances.

External resonances associated with the use of dielectric layers were observed experimentally by Bates[38] and Byron and Frank,[39] experimentally in a phased array waveguide simulator by Hannan,[40] Byron and Frank,[39] and Gregorwich et al,[41] and predicted theoretically by Frazita,[42] Knittel et al,[29] and Parad[43] using one-mode approximations (grating lobe series), and by Galindo and Wu,[44] Wu and Galindo,[45] and Borgiotti[46] using higher-order modal analyses.

In addition to the growing list of blind-spot occurrences, the nature of the phenomenon has become relatively well understood, and some techniques for avoiding or eliminating the difficulties are available.

35. DuFort, E.C. (1968a) Design of corrugated plates for phased array matching IEEE Trans. AP-16:37-46.

36. DuFort, E.C. (1968a) A design procedure for matching volumetrically scanned waveguide arrays, Proc. IEEE 56:1851-1860.

37. Mailloux, R.J. (1972) Surface waves and anomalous wave radiation nulls on phased arrays of TEM waveguides with fences, IEEE Trans. AP-20: 160-166.

38. Bates, R.H.T. (1965) Mode theory approach to arrays, IEEE Trans. and Propagation (Communications) AP-13:321-322.

39. Byron, E.V., and Frank, J. (1968a) Lost beams from a dielectric covered phased-array aperture, IEEE Trans. AP-16:496-499.

40. Hannan, P.W. (1967) Discovery of an array surface wave in a simulator, IEEE Trans. AP-15:574-576.

41. Gregorwich, W.S., Hessell, A., Knittel, G.H., and Oliver, A.A. (1968) A waveguide simulator for the determination of a phased-array resonance, IEEE G-AP International Symposium Digest, 134-141.

42. Frazita, R.F. (1967) Surface-wave behavior of a phased array analyzed by the grating-lobe series, IEEE Trans. AP-15:823-824.

43. Parad, L.I. (1967) The input admittance to a slotted array with or without a dielectric sheet, IEEE Trans. (Communications) AP-15:302-304.

44. Galindo, V., and Wu, C.P. (1968) Dielectric loaded and covered rectangular waveguide phased arrays, Bell System Technical Journal 47:93-116.

45. Wu, C.P., and Galindo, V. (1968) Surface wave effects on dielectric sheathed phased arrays of rectangular waveguides, Bell System Technical Journal 47:117-142.

46. Borgiotti, G.V. (1968) Modal analysis of periodic planar phased arrays of apertures, IEEE Proc. 56:1881-1892.

The initial impression of Allen[47] and Lechtreck,[30, 48] that the null was due to coupling into a surface wave, gave an incomplete picture because the array elements are not reactively terminated and the elements are placed more than one-half wavelength apart, thus eliminating any conventional surface wave propagation. Farrell and Kuhn[32, 33] performed the first rigorous analysis of an array with a blind spot, and they were the first to observe that certain waveguide higher-order modes play a dominant role in achieving the cancellation necessary for a null. Diamond[49] and later Borgiotti[46] confirmed all of these findings for waveguide arrays.

Oliner and Malech[50] suggested what is now generally accepted as true, that the blind spot is associated with the normal mode solution of an equivalent reactively loaded passive array, and that the condition for a complete null on the real array occurs when the elements are phased to satisfy the boundary conditions for the equivalent passive array. Knittel et al[28] developed this theory and showed that in the vicinity of the null the solution corresponds to a leaky wave of the passive structure, but that a surface-wavelike field exists immediately at the null. This is consistent with the results of an analysis made earlier by Wu and Galindo,[45] who demonstrated that the only radiating (fast) wave of the periodic structure spatial harmonic spectrum is identically zero at a null, and that, for this reason, a structure with a period greater than one-half wavelength can have a normal mode. Along with these contributions to the understanding of the physics of a phased array null, a number of authors showed that both the waveguide aperture and lattice dimensions are critical in determining the likelihood of a blind spot.[51-54]

47. Allen, J. L. (1965) On surface-wave coupling between elements of large arrays, IEEE Trans. AP-13:638-639.

48. Lechtreck, L. W. (1968) Effects of coupling accumulation in antenna arrays, IEEE Trans. AP-16:31-37.

49. Diamond, B. L. (1968) A generalized approach to the analysis of infinite planar array antennas, Proc IEEE 56(No. 11):1837-1851.

50. Oliner, A. A., and Malech, R. G. (1964) Speculation on the Role of Surface Waves, Microwave Scanning Antennas, Academic Press, N.Y., Vol. 2, 308-322.

51. Ehlenberger, A. G., Schwartzman, L., and Topper, L. (1968) Design criteria for linearly polarized waveguide arrays, IEEE Proc. 56(No. 11): 1861-1872.

52. Byron, E. V., and Frank, J. (1968b) On the correlation between wideband arrays and array simulators, IEEE Trans. (Communications) AP-16: 601-603.

53. Hessel, A., and Knittel, G. H. (1969) A loaded groundplane for the elimination of blindness in a phased-array antenna, IEEE G-AP International Symposium Digest, 163-169.

54. Knittel, G. H. (1970) The choice of unit-cell size for a waveguide phased array and its relation to the blindness phenomenon, Presented at Boston Chapter Antennas and Propagation Group Meeting.

Figures 5 and 6 illustrate the use of a graphical technique used by Knittel[55] to reveal a direct relation between the blindness effect and the cutoff conditions of the next-higher waveguide mode and lattice mode (grating lobe). Figure 5 shows the locus on a K-β diagram of the blind spot for the array studied by Farrell and Kuhn[32] (denoted F-K on the figure). It is significant that the curve begins at the TE_{20} cutoff for a null at broadside and ends at the intersection of the m = -1, n = -1 and m = -2, n = 0 higher-order grating lobe cutoff loci at maximum scan. The curve never crosses any of these mode cutoff loci, because crossing the TE_{20} cutoff would allow energy to leak back into the waveguides, and crossing the grating lobe cutoff line would allow energy to radiate by means of a grating lobe. In neither case could the passive equivalent array sustain an unattenuated normal mode (unless the odd mode too were reactively terminated). Figure 6 shows that if the waveguide size is reduced and no other dimensions are changed, the TE_{20} cutoff becomes unimportant and the null curve is nearly asymptotic to the grating lobe locus.

These two figures were included to demonstrate the power of this graphical technique for predicting the onset of blindness difficulties. In all other cases shown by Knittel the blindness locus remained nearly asymptotic to the waveguide or grating lobe cutoff loci, whichever occurred at lower frequency. The implication for design is obviously that the null can be avoided by choosing dimensions sufficiently smaller than those for the cutoff conditions.

Certain exceptions to the above conditions can occur; for example, it is possible[56] to have blindness occurring after the onset of a grating lobe if both the main beam and the grating lobe lie in the same element pattern null, but the insight provided by the graphical approach remains the best available guide for design.

Recently, a number of design techniques have been proposed[57] that make use of the data uncovered by these earlier studies and the blindness phenomenon is now considered much less threatening as long as the basic limitations of grating and element size are respected. Studies of waveguide array interaction have become less fashionable and now very few basic efforts are being conducted along these lines.

---

55. Hessel, A., and Knittel, G.H. (1970) On the prediction of phased array resonances by extrapolation from simulator measurements, IEEE Trans. Antennas and Propagation (Communications) AP-18:121-123.

56. Mailloux, R.J. (1971) Blind Spot Occurrence in Phased Arrays – When to Expect It and How to Cure It, AFCRL-71-0428, Physical Sciences Research Papers, No. 462, Air Force Cambridge Research Laboratories.

57. Lee, S.W., and Jones, W.R. (1971) On the suppression of radiation nulls and broadband impedance matching of rectangular waveguide phased arrays, IEEE Trans. AP-19:41-51.

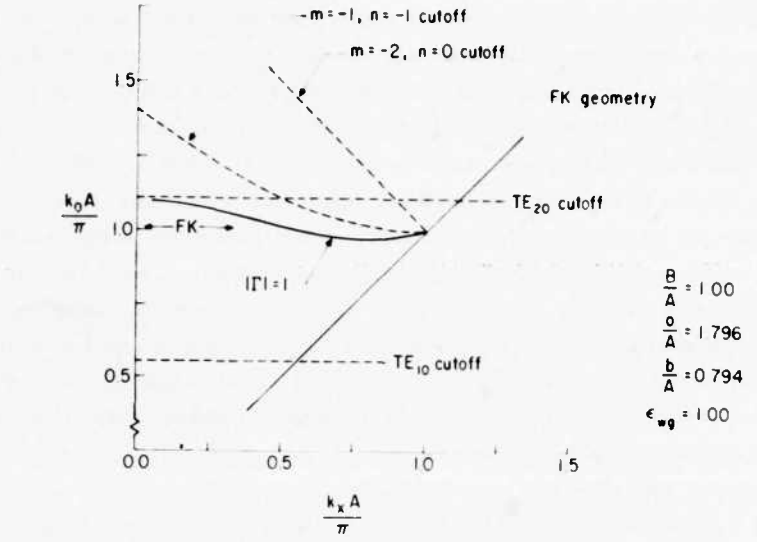

Figure 5. K-β Diagram Showing Null Locus. $\frac{a}{A} = 1.796$
(Courtesy Dr. George Knittel)

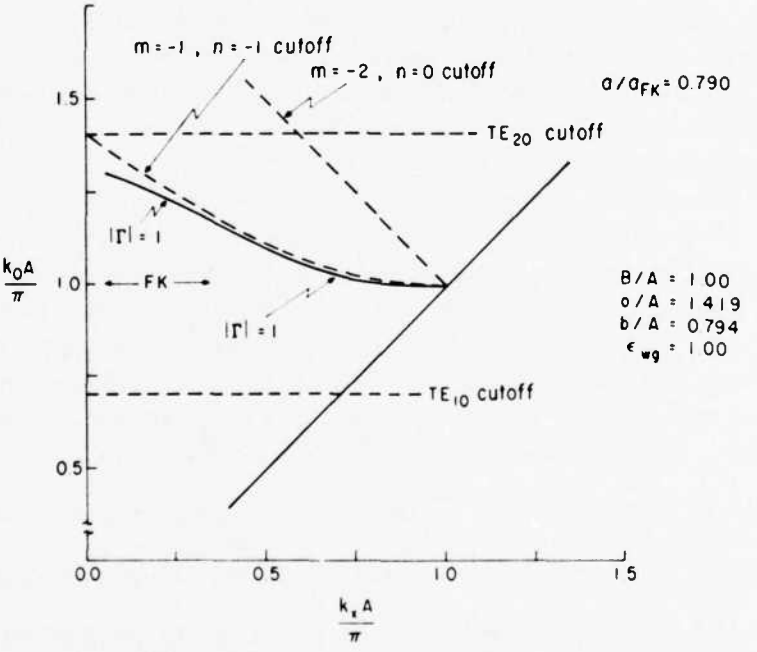

Figure 6. K-β Diagram Showing Null Locus. $\frac{a}{A} = 1.419$
(Courtesy Dr. George Knittel)

Almost all of the studies described above used analytical techniques valid for infinite arrays. Recently, there have also been a number of studies that have included the effects of edges in semiinfinite arrays[11] and finite arrays.[10, 27, 28, 58] These were conducted by assuming single mode aperture fields.

These and other studies too numerous to mention, have brought planar waveguide array theory to an advanced state of development that parallels the present state of dipole array theory. There is peril in assuming that these works mark a reasonable end to analytical studies in waveguide arrays. There remain a multiplicity of problems relating to waveguides conformal to various structures, to wideband and multifrequency waveguides, and to the synthesis of low sidelobe distributions for finite arrays including the mutually coupled terms. These remaining problems are not simple variations of available solutions; they are as varied and general and as fit subjects for research as any other problems in electromagnetic diffraction, and they are more important than most.

Before leaving this generalized history of progress on array boundary value problems, there are several other issues which should be raised. First, the early solutions of the dipole antenna were performed by expanding the dipole current using several judiciously selected distributions,[15] and then forcing the integral equation to be satisfied at the appropriate finite number of points along the dipole. This method is now called "point matching," and has also been used to solve waveguide aperture problems, where the chosen aperture distributions are the waveguide modal fields. More general forms of the method of moments[59] have since achieved substantial success in dealing with wire antenna problems and these have been adapted to aperture problems as well.[60, 61]

Finally in concluding this section on analysis, I should point out that most of the work in the last ten years has dealt with dipoles and waveguides, and so these subjects were highlighted here. We appear to be entering an era of much more generalized radiators, fed by stripline and microstrip and offering a vast, indeed staggering list of boundary value problems that will have crucial impact upon a number of military systems. Some of the beginnings of this technology will be described in succeeding sections of the paper, but as was the case for the waveguide work described here, the technology will be the forcing function and the research

58. Lee, S.W. (1967) Radiation from the infinite aperiodic array of parallel-plate waveguides, IEEE Trans. AP-15(No. 5):598-606.

59. Harrington, R.F. (1967) Matrix methods for field problems, Proc. IEEE 55 (No. 2):136-149.

60. Amitay, N., Galindo, V., and Wu, C.P. (1972) Theory and Analysis of Phased Array Antennas, New York, Wiley-Interscience.

61. Harrington, R.F., and Mautz, J.R. (1975) A Generalized Network Formulation for Aperture Problems, AFCRL-TR-75-0589, Scientific Report No. 8, Contract F19628-73-C-0047.

efforts will be highly directed toward specific problems. Present research funding is not adequate to uncover all of the anomalous behavior with all of the geometries and so research in this important area will be relevant for many years to come and will in many cases be performed in a state of crisis.

3. SPECIAL PURPOSE ARRAYS

3.1 Conformal Arrays and Arrays for Hemispherical Coverage

Aerodynamic requirements for spacecraft and high performance aircraft have stimulated an increasing concern for the design of low profile and conformal antennas. The technological problems of these applications differ, and the technology of conformal arrays is really several technologies. Aircraft fuselage mounted arrays, whether conformal or planar, are expected to provide nearly hemispherical scanning. Spacecraft arrays are sometimes wrapped entirely around the vehicle, and the major design requirement becomes the study of a commutating matrix for steering the beam.[62-65] Arrays on cones have many special problems;[66-68] their radiated polarization is strongly angle dependent, there is little room for the array feed near the tip, and finally, their steering control is necessarily very complex. The specialized problems of an array on a concave surface are discussed in a paper by Tsandoulas and Willwerth.[69]

Common to all of these structures is the underlying fact that they are mounted on nonplanar surfaces, and this alters their radiation and mutual interaction. Analytical treatments have progressed to the rigorous solutions of coupling in

62. Shelley, B. (1968) A matrix-fed circular array for continuous scanning, IEEE Proc. 56(No. 11):2016-2027.

63. Holley, A.E., et al (1974) An electronically scanned beacon antenna, IEEE Trans. AP-22:3-12.

64. Bogner, B.F. (1974) Circularly symmetric r.f. commutor for cylindrical phased arrays, IEEE Trans. AP-22:78-81.

65. Boyns, J.E., et al (1970) Step-scanned circular-array antenna, IEEE Trans. AP-18(No. 5):590-595.

66. Munger, A.D., et al (1974) Conical array studies, IEEE Trans. AP-22:35-43.

67. Hsiao, J.K., and Cha, A.G. (1974) Patterns and polarizations of simultaneously excited planar arrays on a conformal surface, IEEE Trans. AP-22: 81-84.

68. Gobert, W.B., and Young, R.F.H. (1974) A theory of antenna array conformal to surface revolution, IEEE Trans. AP-22:87-91.

69. Tsandoulas, G.S., and Willwerth, F.G. (1973) Mutual coupling in concave cylindrical arrays, Microwave Journal 16(No. 10):29-32.

infinite arrays or slits on cylinders[70, 71] and on conical surfaces.[72] Simpler formulations have been developed using extensions of the geometrical theory of diffraction,[73-75] and with these it is now possible to perform analytical studies of finite arrays on generalized conformal structures. Figures 7 and 8 show results obtained by Steyskal[75] for the reflection coefficient of the center element in an array of 156 dielectric loaded circular waveguides mounted on a cylinder of 11.6λ diameter for the two principal polarizations. Analytical results of this sort can be applied for sylinders with radii of 2λ or greater.

Studies of arrays on cylinders and designed for nearly hemispherical scan coverage[71, 76] have emphasized the difficulty in using conventional array approaches for such wide angle scan. By matching the array near the horizon (say 80° from

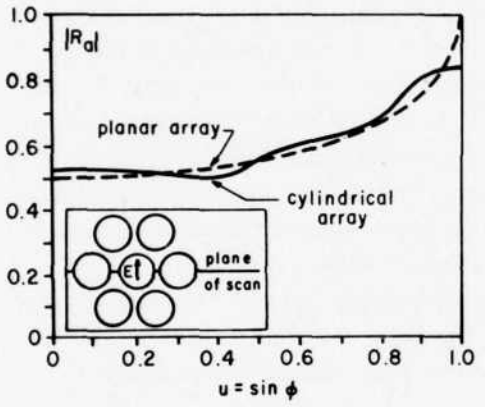

Figure 7. Conformal Array Active Reflection Coefficient H-Plane Scan

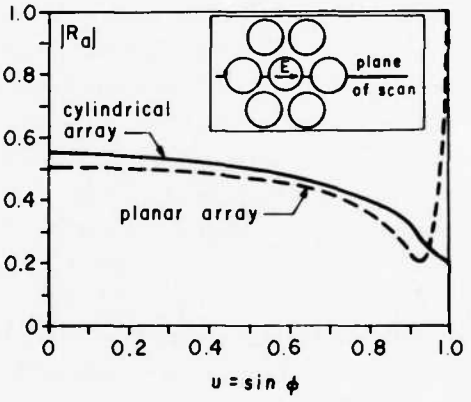

Figure 8. Conformal Array Active Reflection Coefficient E-Plane Scan

70. Borgiotti, G. V., and Balzano, Q. (1970) Mutual coupling analysis of a conformal array of elements on a cylindrical surface, Trans. IEEE AP-18: 55-63.

71. Borgiotti, G. V., and Balzano, Q. (1972) Analysis of element pattern design of periodic array of circular apertures on conducting cylinders, IEEE Trans. AP-20:547-553.

72. Balzano, Q., and Dowling, T. B. (1974) Mutual coupling analysis of arrays of aperture on cones (Communications), IEEE Trans. AP-22:92-97.

73. Golden, K. E., et al (1974) Approximation techniques for the mutual admittance of slot antennas in metallic cones, IEEE Trans. AP-22:44-48.

74. Shapira, J., et al (1974) Ray analysis of conformal array antennas, IEEE Trans. AP-22:49-63.

75. Steyskal, H. (1974) Mutual coupling analysis of cylindrical and conical arrays, IEEE/AP-S Int. Symp. Record, 293-294.

76. Maune, J. J. (1972) An SHF airborne receiving antenna, Twenty Second Annual Symposium on USAF Antenna Research and Development.

the zenith), the array can be made to have gain variation of only about 6 dB over the hemisphere but the array matched at this angle is mismatched at other scan angles, and can suffer a gain reduction of up to 4 dB at broadside.[76] Recent studies sponsored by RADC/ET have demonstrated coupling into a surface-wave mode or operation for near-endfire radiation. These efforts[77, 78] have included the use of dielectric structures over or in the vicinity of the array, and have shown that these means also improve gain coverage within the hemisphere so that the envelope of peak radiation gain is always within about 6 dB of the maximum radiation over a narrow frequency range. Computations[78] have shown that the coverage obtainable from an array with 23 dB nominal gain presents maximum oscillations of 8 dB over a 10-percent bandwidth. This data was obtained for an array covered with a layer of $C_r = 4$ material 0.075λ thick extending over and beyond the array. Such wide angle scanning does not seem feasible at present for arrays with 30 dB gain.

Inhouse studies at RADC/ET have used the array in a conventional manner except at endfire where coverage is provided by short circuiting the array elements to form a corrugated surface that can support a surface wave for endfire radiation. This technique can provide highly efficient radiation over a hemisphere for one plane of scan, but is also gain limited at about 20 dB for a square array.

Figure 9 shows an array of 64 waveguide elements excited by an 8 element feed. Although not shown in the figure, the array is also excited by a 64 way power divider and 8 phase shifters to form a beam scanned in the elevation plane. In practice, the waveguides would be short circuited by diodes or mechanical shorting switches to form the corrugated surface for endfire radiation, but the experiment was conducted using fixed short circuits.

The groundplane, partially shown in Figure 9, measured 6-ft wide and had a 4-ft curved surface with 84-inch radius extending in front of the antenna structure.

Figure 10 shows the measured array gain at 9.5 GHz for a number of beams within the sector including a beam scanned to the horizon and one formed by the excited corrugated structure. A cosine envelope distribution is also included for reference. The data show that the surface wave beam provides approximately 6 dB gain increase at the horizon as compared with the scanned endfire beam, and that in fact the achievable gain at the horizon is 17 dB; only 4 dB below the maximum,

---

77. Villeneuve, A.T., Behnke, M.C., and Kummer, W.H. (1973) Hemispherically Scanned Arrays, AFCRL-TR-74-0084, Contract No. F19628-72-C-0145, Scientific Report No. 2. Also, see 1974 International IEEE AP-S Symposium Digest, 363-366.

78. Balzano, Q., Lewis, L.R., and Siwiak, K. (1973) Analysis of Dielectric Slab-Covered Waveguide Arrays on Large Cylinders, AFCRL-TR-73-0587, Contract No. F19628-72-C-0202, Scientific Report No. 1.

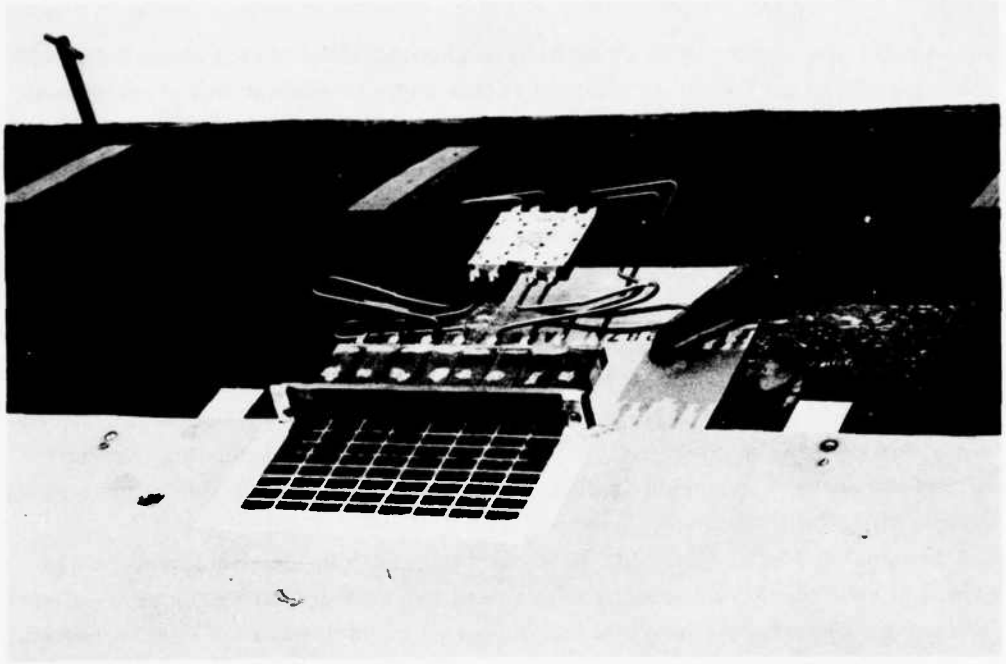

Figure 9. Waveguide Array Used in Hemispherical Scan Experiments

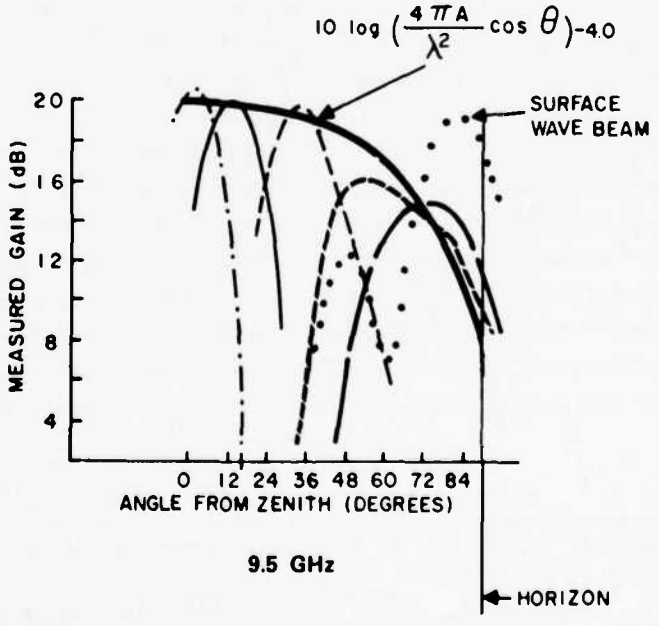

Figure 10. Scan Data for Hemispherical Scan Array at 9.5 GHz

and the peak at 80° is nearly equal to the broadside gain. The minimum of the pattern gain envelope occurs at about 69°, and shows a dip down to approximately 15 dB which is within about 1 dB of the array projection factor (cos θ).

These studies are but the beginning of the necessary research to develop flush mounted aircraft antennas that can be scanned over the entire hemisphere. This research is crucial because of the potential for substantially reduced antenna size and lower cost. Its importance is understood by realizing that there is a vast number of aircraft intended to have SHF communications links by the mid-1980's, and present antenna technology requires overdesign by nearly 10 dB. It is difficult to overestimate the importance of research in this extremely difficult technical area.

For a number of applications, a flat array offers no advantage over a cylindrical or spherical array. In such situations, it is better to avoid the natural disadvantages of the flat array and use the vertical projection of a structure with curved front face to achieve some increased gain at the horizon. This is done to an extent in some of the cylindrical array studies but the Dome[79, 80] antenna capitalizes upon this projection in a way that no other system does. This basic antenna, shown in Figure 11 uses a passive, spherical lens to extend the scan coverage of a conventional planar array to hemispheric coverage or greater. Each dome module consists of a collector element, a fixed delay, and a radiator element. The dome assembly is radiated by the feed array, a conventional electronically scanned space fed lens with an F/D of 0.75. The array generates a nonlinear phase front to steer the dome from zenith to and somewhat below the horizon. Although some sacrifice in array efficiency is traded for wide angle scanning, the dome scan characteristics can be tailored to optimize the radiation over desired subsectors. Examples quoted in the literature show experimental results for a dome with phase shift modules chosen to form two different gain scan contours; one with a peak at 60° from zenith, and one at 120° from zenith. Such flexibility of selection allows this technique to become a reasonable choice for a number of system applications; it will continue to be of importance as a subject for research and development in order to improve efficiency, bandwidth, and sidelobe levels and so achieve optimized designs for a number of specialized requirements.

---

79. Schwartzman, L., and Stangel, J. (1975) The dome antenna, Microwave Journal 18(No. 10):31-34.

80. Esposito, F.J., Schwartzman, L., and Stangel, J.J. (1975) The Dome Antenna-Experimental Implementation, URSI/USNC Meeting Digest 1975, June 3-5, Commission 6.

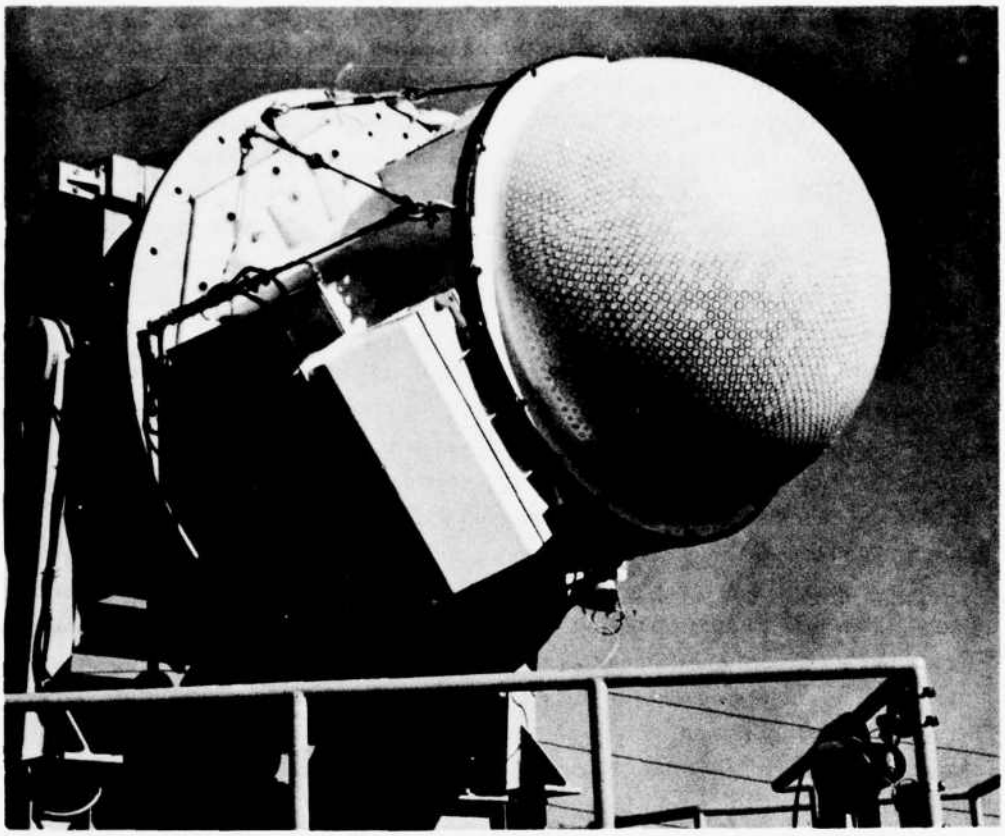

Figure 11. The Dome Antenna: A Technique for Hemispherical Scan

3.2 Low Sidelobe and Null Steered Arrays

Among the areas of prime interest in radar and special purpose arrays are the requirements of providing low sidelobe and null steered radiation patterns. These two concerns have grown, because of the military threats presented by ARM (Ant-Radiation Missiles) and the increased use of jammers. Obviously, the solution is just to use the well-known aperture distributions that have low sidelobe Chebyshev or Taylor pattern functions and so reduce sidelobes to the theoretical limits; but this solution seldom is applicable except to certain broadside arrays or

slot arrays with fixed beam positions. Studies[81-84] of random phase and amplitude effects and of pattern distortion due to phase quantization have led to statistical predictions of sidelobe levels for fixed beam and scanned arrays.

Another problem that limits the sidelobe ratio maintainable by an array is that the element pattern $f_m(\theta, \phi)$ differs for each element "m" in an array. Equation (31) gives a general expression for this complex function and shows that it depends upon all of the mutual coupling terms from everywhere in the array, and so only the elements near the array center have the same element patterns. The patterns for elements near the array edges are not only different in amplitude, but can have different spatial dependence than those for central elements. This means that any amplitude weighting specified for sidelobe suppression must vary with scan angle to achieve the lowest possible sidelobes. Problems of this sort have caused little concern in the past because edge effects are not dominant in large radar arrays, and because it has become common practice to leave a number of unexcited elements near the edges of these arrays so that the excited elements have more similar element patterns. Specifying extremely low sidelobes for small arrays may cause this problem area to grow until it poses a fundamental limitation on array performance. As yet there has been little research expended on this potentially troublesome area, but as better phase shifters and more accurate power division schemes become available, element pattern distortion will remain as the dominant limitation on sidelobe reduction for small arrays.

Among the more important areas of array research is the topic of pattern null steering to eliminate jamming interference. Most recent contributions to this subject[85, 86] have included consideration of mutual coupling effects and proceed from an equation similar to Eq. (31). Assuming only one mode in each aperture ($Q = 1$), Eq. (31) is written:

---

81. Ruze, J. (1952) Physical Limitations on Antennas, MIT Research Lab. Electronics Tech. Rept. 248.

82. Miller, C.J. (1964) Minimizing the effects of phase quantization errors in an electronically scanned array, Proc. 1964 Symp. Electronically Scanned Array Techniques and Applications, RADC-TDR-64-225, Vol. 1, 17-38, AD448421.

83. Allen, J.L. (1960, 1961) Some extensions of the theory of random error effects on array patterns, in J. L. Allen et al., Phased Array Radar Studies, Tech. Rept. No. 236, Lincoln Laboratory, M.I.T.

84. Elliott, R.S. (1958) Mechanical and electrical tolerances for two-dimensional scanning antenna arrays, IRE Trans. AP-6:114-120.

85. McIlvenna, J.F., and Drane, C.J. (1971) Maximum gain, mutual coupling and pattern control in array antennas, The Radio and Electronic Engineer, 41(No. 12):569-572.

86. McIlvenna, J., et al (1976) The Effects of Excitation Errors in Null Steering Antenna Arrays, RADC-TR-76-183, Rome Air Development Center.

$$F(\theta,\phi) = \gamma_1 I_1(\theta,\phi)\, j\omega \sum_{m=1}^{M} e^{jk_o(ux_m+vy_m)} a_m \left[1 + \sum_{n=1}^{M} S_{mn}\right]$$

$$= \gamma_1 I_1(\theta,\phi)\, j\omega C^T e \qquad (32)$$

where $C = (S + I)\, a$, a is a column vector of excitations, and I is the $M \times M$ — element identity matrix:

$$a = \begin{pmatrix} a_1 \\ a_2 \\ \cdot \\ \cdot \\ \cdot \\ a_M \end{pmatrix} \qquad C = \begin{pmatrix} C_1 \\ C_2 \\ \cdot \\ \cdot \\ \cdot \\ C_M \end{pmatrix}$$

and (33)

$$e = \begin{bmatrix} e^{jk_o(ux_1+vy_1)} \\ \cdot \\ \cdot \\ \cdot \\ e^{jk_o(ux_M+vy_M)} \end{bmatrix}$$

and

$$C^T = a^T (S + I)^T \quad .$$

The power pattern has the form

$$P(\theta,\phi) = F(\theta,\phi) \cdot F^*(\theta,\phi)$$

$$= |\gamma_1^2|\, |I_1^2(\theta,\phi)|\, \omega^2 [C^+ (e \cdot e^+) C] \qquad (34)$$

$$= |\gamma_1^2|\, |I_1^2(\theta,\phi)|\, \omega^2 a^+ [(I + S)^+ e\, e^+ (I + S)]\, a$$

where the symbol + denotes the combined transpose and complex conjugate operations.

Thus:

$$P(\theta, \phi) = |\gamma_1^2| \; |I_1^2(\theta, \phi)| \; \omega^2 (a^+ \bar{A} \, a) \tag{35}$$

where

$$A = (I + S)^+ \, e \, e^+ (I + S)$$

is a one term dyad.

The directive gain is defined as the ratio of this $P(\theta, \phi)$ to the total radiated power P_R, which is given by:

$$P_R = a^+ (I - S^+ S) \, a \quad . \tag{36}$$

Thus a normalized quadratic form for directive gain, in terms of the scattering matrix $\bar{S}$, assuming single mode excitation and only single mode contributions present in the far field radiation expansion is:

$$G(\theta, \phi) = |I^2(\theta, \phi)| \; \frac{a^+ A \, a}{a^+ B \, a} \tag{37}$$

where

$$B = I - S^+ S \quad .$$

This expression for gain is a quadratic form. It could include the computed or measured scattering matrix data, and is a convenient form for optimizing subject to various constraints. Some details of an appropriate optimization are given in the literature,[85, 86] and a recent report illustrates[86] and details the specific procedure used for optimizing the directive gain of the single mode waveguide array problem described above. The procedure has been applied in a number of situations for dipole and waveguide arrays with finite numbers of elements and including mutual coupling. It has never been applied to situations that included important higher order mutual coupling expressions. Of particular importance is that the numerics of the problem becomes simpler as the number of constraints are increased. Thus this sort of optimization has been used to place a number of nulls close together within a sector of a pattern, and so produce a trough that would eliminate the effects of narrowband jammers over a relatively wide spatial sector. The recent study[86] addresses the effects of random errors in phase and amplitude

control on null and trough formation, and concludes that 0.1 dB of amplitude and 1^{o} rms of phase control are necessary to maintain a -40 dB trough. When phase shifters, power dividers, and engineering practices allow such, required tolerances can be obtained; then again the fundamental technical problem of higher order radiating fields will remain and assume its dominance as the ultimate limit to radiation suppression.

Techniques like the one mentioned above imply that good amplitude control is available in addition to the required phase control. This is seldom the case, and has been the major factor hindering the advance of technology based upon such optimization. The increasing importance of antijamming protection will, however, make these systems the subject of intensified research interest as pressures increase to simplify feed networks and broaden system bandwidth. Several other options for antijam array techniques will be discussed in subsequent sections of the paper.

3.3 Array Techniques for Limited Sector Coverage

One of the most important classes of special purpose array techniques are those which trade scan capability for decreased cost. These are called "limited scan arrays," and they exist because there are many military and civilian requirements for high gain, electronically scanned antennas that need scan only some restricted sector of space. Military requirements include weapons locators, antennas for synchronous satellites and for air traffic control. Civilian requirements are mainly for air traffic control.

Two general classes of arrays are used for limited scan systems; the first class, which is historically the earliest and the most successful, is an array that is placed in or near the focal region of a reflector or lens antenna to scan its beam. The second class consists of large aperture elements and a beam forming network that includes some means of suppressing the system grating lobes. In either case, there exists a minimum number of control elements that are required for beam scanning over any given sector and this serves as one measure of the efficiency of the scanning system.

One measure of this minimum number is the number of orthogonal beams within the scan sector. Another is the theorem of Stangel[87] which states that the minimum number of elements is:

$$N = \frac{1}{4\pi} \oiint G_o(\theta, \phi)\, d\Omega \qquad (38)$$

87. Stangel, J.J. (1974) A basic theorem concerning the electronic scanning capabilities of antennas, URSI Commission VI, Spring Meeting.

where $G_o(\theta, \phi)$ is the maximum gain achievable by the antenna in the (θ, ϕ) direction, and $d\Omega$ is the increment of solid angle.

Another measure of the minimum number of array elements is contained in the definition of a parameter introduced by Patton[88] and called the "element use factor." This parameter will be used in a somewhat generalized form to compare the number of phase shifters in competing systems with unequal principal plane beamwidths. The factor is N/N_{min} where N is the actual number of phase shifters in the control array, and N_{min} is a reasonable number of control elements as defined below:

$$N_{min} = \left(\frac{\sin \theta^1_{max}}{\sin \frac{\theta^1_3}{2}} \right) \left(\frac{\sin \theta^2_{max}}{\sin \frac{\theta^2_3}{2}} \right) . \tag{39}$$

θ^1 and θ^2 max are the maximum scan angles in the two orthogonal principal planes measured to the peak of each beam, and θ^1_3 and θ^2_3 are the half power beamwidths in these planes. Thus N - min is approximately four times the product of the number of beamwidths scanned in each principal plane, and as will be shown later, is also approximately equal to the number of orthogonal beam positions for a rectangular array with beams filling a rectangular sector in direction cosine space. Although more general, Stangel's formula reduces to Patton's in the limiting case of small scan angle and using the approximate formula

$$G_o = \frac{4\pi}{\theta^1_3 \theta^2_3} \tag{40}$$

and integrating over a rectangular sector.

In the case of a periodic array with a square or rectangular grid, the condition of the minimum phase controls can be shown to require that the following relation be satisfied in each plane:

$$\left(\frac{d}{\lambda}\right) \sin \theta_{max} \leq 0 . \tag{41}$$

88. Patton, W.T. (1972) Limited scan arrays, in Phased Array Antennas; Proc of the 1970 Phased Array Antenna Symposium, edited by A.A. Oliner and G.H. Knittel, Artech House, Inc., MA., 332-343.

A more recent study by Borgiotti[89] describes a similar bound and presents a technique for synthesizing patterns with various sidelobe levels that satisfy the criterion of requiring a minimum number of controls.

Given that there is a minimum number of required controls for any given sidelobe level, beamwidth and scan or multiple beam coverage sector, the remaining issue is to investigate techniques for optimizing scanning systems, subject to given sidelobe requirements, so that their characteristics approach those of an ideal scanner.

Optical techniques that combine single or dual reflectors or lenses with phased arrays to achieve sector scanning have the advantage that they have grown out of techniques for large apertures and so naturally provide high gain. Alternatively, the array techniques that have existed in the past lend themselves to much greater control of aperture distributions for sidelobes, but are not so readily suited to the high gain requirements of present systems for limited scan coverage. Cost factors and the availability of technology have brought about an intense period of creative engineering that has resulted in the current state of optical feed limited scan systems.

Design of this class of systems is dominated by optical considerations, and problems of spill-over, aperture blockage, off axis focusing, and induced cross polarization often effect the design more than the ratio of beam positions to control elements. Aperture efficiency is another parameter of importance for many applications. Many of the reflector or lens geometries require oversize apertures because the feed structure illuminates only a spot on the main aperture, and that spot moves with scan angle. For these devices, aperture efficiencies can be of the order of 25 percent instead of the usual 55 to 60 percent for nonscanning reflectors, and so scanning reflectors or lenses often require double the aperture of the more efficient fixed beam structures. The type of beam steering required is also a factor of great importance; the simplest being row and column steering with progressive phases in both planes. Certain antennas, however, require complex steering functions for off axis scans, and these result in slower beam steering and larger computer data storage.

Optical limited scan techniques have their origin in the development of mechanically scanned reflector and lens geometries using feed tilt[90] and displacement,[91] and in the development of feeds to correct the wide angle performance of beam

89. Borgiotti, G. (1975) Design Criteria and Numerical Simulation of an Antenna System for One-Dimensional Limited Scan, AFCRL-TR-75-0616.

90. Silver, S., and Pao, C. S. (1944) Paraboloid Antenna Characteristics as a Function of Feed Tilt, MIT Radiation Lab., Cambridge, MA, Rep 479.

91. Ruze, J. (1965) Lateral feed displacement in a paraboloid, IEEE Trans. Antennas Propagation AP-13:660-665.

shaping reflectors.[92] Present devices include single and dual reflection of lens geometries in combination with a phased array, that produce an electronically scanned beam using relatively few phase controls.

Design principles for such a wide ranging collection are themselves so varied that they cannot be developed from basic principles in a text of this length. Instead, this paper will outline some of the more important contributions to the technology and to the analytical and conceptual tools that made the technology possible. Several recent sources include comprehensive surveys of developments in these areas.[93, 94]

Many of the early studies on mechanical scanners were performed using geometrical optics, and even today this method receives wide usage for computing required feed locations, focusing conditions and phase shifter controls, and for investigating general design parameters. Recent studies[94] have emphasized the deficiencies of the geometrical optics approach for obtaining intensity information about focal region fields and have demonstrated the use of physical optics for design. Analytical methods used in design are noted in the descriptions that follow.

Early studies of scanning parabolas have uncovered a number of useful design concepts. Using ray optical techniques, Sletten et al,[92, 93] have investigated the location of focal (or caustic) surfaces for paraboloidal reflectors receiving off axis plane waves, and have shown how these characteristics can be used to develop midpoint correctors for elevation beam shaping while maintaining a narrow focused beam in the azimuthal plane, and ridege line correctors for forming several pencil beams in elevation without destroying azimuthal focus. Ruze[91] has used a scalar plane wave theory to analyze the scanning characteristics of a parabola with a laterally displaced feed located at the Petzval surface. This analysis was used to obtain scanning patterns, to evaluate coma-lobe contributions and to derive equations for the number of beamwidths scanned by such displacement for a -10.5 dB coma lobe at the scan limit. This number is given below as

$$N = 0.44 + 22(f/D)^2 \quad .$$

Recent work by Rusch and Ludwig[94] has included a numerical evaluation of focal region fields for a paraboloid receiving an off axis plane wave. Results of

92. Sletten, C.J., et al (1958) Corrective line sources for paraboloids, IEEE Trans. AP-6(No. 3):239-251.

93. Collin, R.E., and Zucker, F.J. (1969) Antennas Theory, Part 2, McGraw-Hill Book Co., New York, Chapter 17.

94. Rusch, W.V.T., and Ludwig, A.C. (1973) Determination of the maximum scan-gain contours of a beam-scanning paraboloid and their relation to the pitzval surface, IEEE Trans. Antennas Propagation, AP-21:141-147.

this study show that the maximum focal field locus, and therefore the position of optimum feed location, does not coincide with the Petzval surface, but remains relatively close to it for low f/D values. Reflectors with f/D greater than 0.5 have their optimum feed location closer to the focal point than the Petzval surface, but this location tends toward that line for large scan angles.

Imbriale et al[95] have also considered parabolic reflectors with large lateral feed displacements, and have compared the results of Ruze's scalar theory with the complete vector theory solution and experimental data for various feed displacements. This study demonstrated that the coma-lobe level is sometimes vastly underestimated by the scalar theory when used for feeds with large displacement.

Another recent work of significant import has been reported by Rudge[96] who has demonstrated the spatial fourier transform relationship between the aperture fields of a parabolic reflector and its focal plane fields. In an extension of this work, Rudge and Withers have also shown[97, 98] that the fields in a specified off axis focal plane bear the same transform relationship to the aperture field under the excitation of an inclined wave.[99]

Not surprisingly, the first viable limited scan antennas consisted of a parabolic reflector[100] with an array placed between the reflector and the focal point as shown in Figure 12. The array is then required to produce the complex conjugate of the field that it would receive from a distant point source at a given angle, and the extent to which it can do this determines the quality of the antenna radiation pattern. Because of the complexity of the converging field, White and DeSize[101] placed an array of feeds on a spherical surface concentric with the parabola focal point, and demonstrated scanning for that case. More recent structures do use parabolas with nonlinear phase controls in the array, and achieve sidelobes at the -18 to

---

95. Imbraile, W.A., et al (1974) Large lateral feed displacements in a parabolic reflector, IEEE Trans. AP-22(No. 6):742-745.

96. Rudge, A.W. (1969) Focal plane field distribution of parabolic reflectors, Electronics Letters 5:610-612.

97. Rudge, A.W., and Withers, M.J. (1971) New techniques for beam steering with fixed parabolic reflectors, Proc. IEEE 118(No. 7):857-863.

98. Rudge, A.W., and Withers, M.J. (1969) Beam-scanning primary feed for parabolic reflectors, Electronic Letters 5:39-41.

99. Rudge, A.W., and Davies, D.E.N. (1970) Electronically controllable primary feed for profile-error compensation of large parabolic reflectors, Proc. IEEE 117(No. 2):351-358.

100. Winter, C. (1968) Phase scanning experiments with two reflector antenna systems, Proc. IEEE 56(No. 11):1984-1999.

101. White, W.D., and DeSize, L.K. (1962) Scanning characteristics of two-reflector antenna systems, 1962 IRE International Conv. Record, Pt. 1, 44-70.

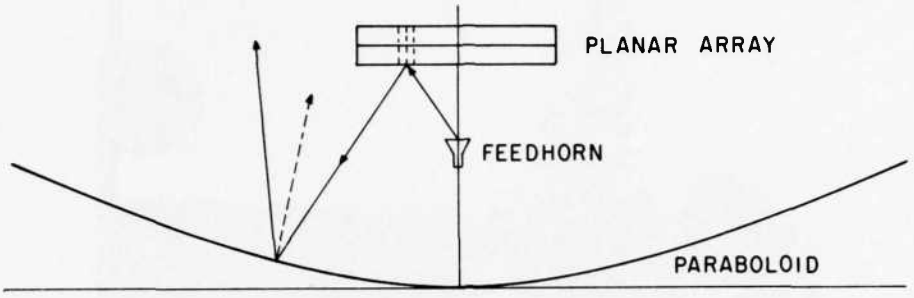

Figure 12. Reflector/Array Combination for Limited Sector Coverage

-20 dB level. Examples of these structures are the AGILTRAC antenna[102, 103] and the AN/TPN-19 Precision Approach Radar Antenna (Figure 13). One final example of a single reflector or lens geometry scanned by a phased array is shown in Figure 14. This antenna differs fundamentally from the other optical schemes because the main reflector or lens is not restricted by a focusing condition. This new concept in limited scan antennas, proposed by Schell,[104] uses an array disposed around a cylinder to scan a reflector or lens surface that is contoured according to an optimum scan condition, rather than a focusing condition. The reflector is then stepped or the lens phase corrected to achieve focusing. Preliminary design results[105] show that in one plane of scan the technique achieves an element use factor of about unity, while using an oversize final aperture to again allow motion of the illuminated spot.

Figure 14 shows a schematic view of the array-lens combination and Figure 15 demonstrates its scanning properties. The array element corrents are equal in amplitude and have a progressive phase given by $\beta n \Delta\theta$. The reflector surface (or lens back face) is chosen to transform this phase variation into a linear wavefront normal to the beam direction. The condition for determining the curvature of the reflector (or lens) is that a constant incremental phase change in θ along the

102. Tang, C. H. (1970) Application of limited scan design for the AGILTRAC-16 antenna, 20th Annual USAF Antenna Research and Development Symposium, University of Illinois.

103. Howell, J. M. (1974) Limited Scan Antennas, IEEE/AP-S International Symposium.

104. Schell, A. C. (1972) A Limited Sector Scanning Antennas, IEEE G-AP International Symposium.

105. McGahan, R. (1975) A Limited Scan Antenna Using a Microwave Lens and a Phased Array Feed, M. S. Thesis, MIT.

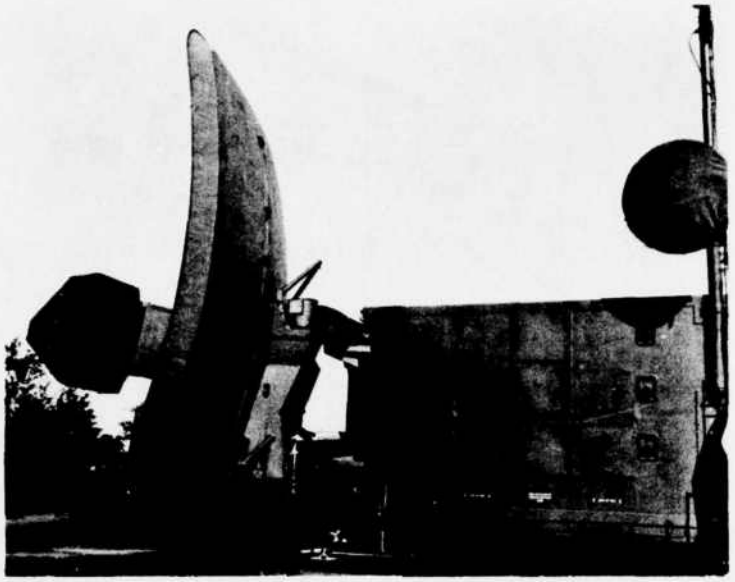

Figure 13. Precision Approach Radar Antenna AN/TPN-29

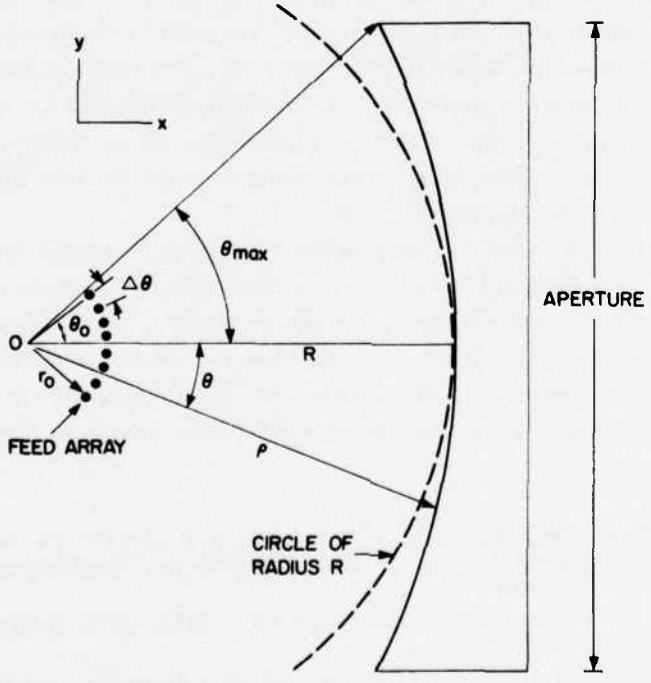

Figure 14. Scan Corrected Lens Antenna

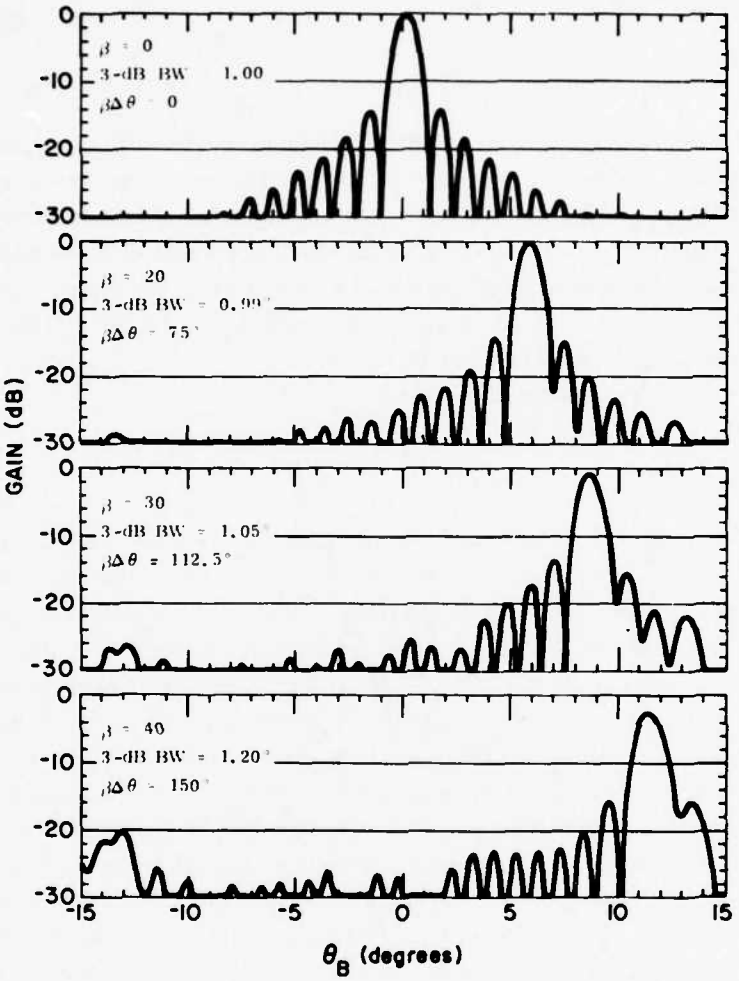

Figure 15. Pattern Characteristics of Scan Corrected Lens

circular arc tangent to the center of the back face of the lens, produces a constant incremental phase change in the "y" coordinate along the aperture.

Thus

$$\frac{dy}{d\theta} = \text{Constant} = R \tag{42}$$

and, since $y = \rho \sin \theta$

$$\rho = \frac{R\theta}{\sin \theta} \quad . \tag{43}$$

This curvature satisfies the scan requirement, but does not guarantee that the wave will focus. Focusing is achieved for the reflector through the use of confocal parabolic sections stepped so that their centers lie along the scan surface, and for the lens by adjusting the path lengths so that they are equal at some angle. The array represented by the data of Figure 15 consists of 25 elements. The half angle θ_o subtended by the array is 45^o, $k_oR = 197$, $k_oa = 48$ and k_o times the final aperture width is approximately 526 ($D/\lambda = 83.7$).

The far field beam angle is given by

$$\sin \theta_B = \beta/kR \quad , \tag{44}$$

and for the case shown in the figure the maximum θ_B is about 11.5^o. At this scan angle the gain is reduced about 2.5 dB with respect to broadside and a far-sidelobe has risen to the -20 dB level. The aperture illumination is nearly uniform, and the -13 dB near sidelobe ratio is maintained throughout the scan sector.

These computations by McGahan[105] have been confirmed experimentally for the lens geometry scanning in one plane. An element use factor of 0.95 would result if the same economy of phase controls can be maintained for the lens scanning in two dimensions. Since the amplitude distribution on the array is transferred very simply onto the inner lens surface, it is possible to produce very low sidelobe patterns with this geometry. Preliminary theoretical data indicate that with perfect phase and amplitude control this structure can have sidelobes below -40 dB.

Single reflector or lens structures with a phased array feed are simple but, with the exception of the technique described by Schell and McGahan, they require a relatively large number of phase controls (element use factors of 2.5-3.25). All of these antennas require oversize main apertures because the illumination moves with scan (typical aperture efficiencies are 20-25 percent). Thus large aperture size coupled with weight and cost limitations, usually restricts the choice of final aperture to that of a reflector, and the resulting blockage can cause sidelobe problems and the need for offset feeds.

Studies of dual reflector of lens combinations illuminated by a phased array have followed two distinct paths. One class has used relatively small subreflectors, linear progressive phase control but comparatively large element use factors because the array cannot be used optimally. The small subreflector requires that the array scan sector be limited, and if the array is not designed to take advantage of this fact, then the element use factor will be larger than the theoretical minimum.

Examples of this first category are the near field cassegrain geometry and the offset fed gregorian geometry of Fitzgerald.[106, 107, 108] The second category of dual reflector or lens scanning antennas uses a much larger secondary aperture and an array that scans over wide angles. This type of antenna can have element use factors close to unity, but the required secondary aperture sizes make the structure bulky. Comparison of two antennas in this category[109, 110] with the Fitzgerald studies indicate that element use factors of 1.4 can be maintained using secondary apertures of approximately 0.7 the diameter of the main reflector, but restricting the subreflector size to 0.35 to 0.25 of the main reflector diameter led to element use factors of between 2.5 and 4. Larger subreflectors also allow more accurate control of the main reflector illumination and in one case[110] resulted in approximately -20 dB sidelobes over the scan sector.

In addition to these combinations of array and optical structures, there is a growing class of antennas that scan efficiently over limited sectors using novel array techniques. Each achieves its relatively low cost by using large array elements or subarrays and so reducing the number of required phase controls for a given size final aperture. This use of oversize elements in a periodic array results in grating lobes, which are suppressed by careful control of the subarray element pattern, or by scanning the element patterns to null certain of the lobes. Alternatively, other approaches have used pseudorandom array grids to reduce the peak levels of the grating lobes by redistributing their energy over a wider sector of space.

The radiated field of the array of aperture elements shown in Figure 1 given in direction-cosine space for a beam at (u_o, v_o) is:

$$E(u, v) = \frac{e(u, v)}{N} \sum_{m=1}^{N_x} \sum_{n=1}^{N_y} A_{mn} e^{j\frac{2\pi}{\lambda}(umd_x + \Delta_n u + vnd_y)} \tag{45}$$

---

106. Fitzgerald, W. D. (1971) Limited Electronic Scanning with an Near Field Cassegrainian System, ESD-TR-71-271, Technical Report 484, Lincoln Laboratory.

107. Fitzgerald, W. D. (1971) Limited Electronic Scanning with an Offset-Feed Near-Field Gregorian System, ESD-TR-71-272, Technical Report 486, Lincoln Laboratory.

108. Miller, C.J., and Davis, D. (1972) LFOV Optimization Study, Final Report No. 77-0231, Westinghouse Defense and Electronic Systems Center, System Development Division, Baltimore, Md., ESD-TR-72-102.

109. Tang, C.H., and Winter, C.F. (1973) Study of the Use of a Phased Array to Achieve Pencil Beam over Limited Sector Scan, AFCRL-TR-73-0482, ER 73-4292, Raytheon Co., Final Report Contract F19628-72-C-0213.

110. Tang, E., et al (1975) Limited Scan Antenna Technique Study, Final Report, AFCRL-TR-75-0448, Contract No. F19628-73-C-0129.

where

$$u = \sin\theta\cos\phi$$

$$v = \sin\theta\sin\phi$$

and

$$A_{mn} = I_{mn}\, e^{-j\frac{2\pi}{\lambda}(u_o m d_x + u_o \Delta_n + v_o n d_y)} \quad .$$

Here A_{mn} is the signal at the element (m, n) located at the position $x = md_x + \Delta_n$, $y = nd_y$ as required to form the beam at (u_o, v_o). I_{mn} is the signal amplitude and e(u, v) is the element pattern of each aperture in the array. $N = N_x N_y$ is the number of elements in the array.

Assuming that the array is excited by a separable distribution so that $I_{mn} = I_m^H I_n^E$, and assuming that the element pattern is also separable, then $e(u, v) = e_x(u)e_y(v)$ and this field distribution can be written in the following form:

$$E(u, v) = \frac{1}{N_x}\left\{\sum_{m=1}^{N_x} I_m^H\, e_x(u)\, e^{j\frac{2\pi}{\lambda}(u-u_o)md_x}\right\}$$

$$\cdot\, \frac{1}{N_y}\left\{\sum_{n=1}^{N_y} I_n^E\, e_y(v)\, e^{j\frac{2\pi}{\lambda}[(v-v_o)nd_y + \Delta_n(u-u_o)]}\right\} \qquad (46)$$

$$= E_x(u)E_y(u, v) \quad .$$

This pattern is not separable in general, but may be so for certain choices of (Δ_n). The choice of optimum (Δ_n) for grating lobe reduction will be considered later.

If the rows are not displaced, then the field is fully separable and the exponential forms in the above summations have principal maxima at the grating lobe locations:

$$u_p = u_o + \frac{p\lambda}{d_x}$$

$$v_q = v_o + \frac{q\lambda}{d_y} \qquad (47)$$

for all p · q bounded by the inequality

$$K_{pq} = \frac{2\pi}{\lambda}\sqrt{1 - u_m^2 - v_n^2} \leq \frac{2\pi}{\lambda} \quad .$$

These points are shown in (u, v) space as a regularly spaced grating lobe lattice about the main beam location (u_o, v_o) in Figure 16. The circle with unity radius represents the bounds of the above inequality; all grating lobes within the circle represent those radiating into real space, and those outside do not radiate.

Figure 17 shows how the array factor and element pattern combine to produce the resulting radiated distribution in one principal plane. This figure illustrates how the effects of squinting or narrowing the element pattern or of destroying the periodicity can serve to reduce resulting grating lobes by altering either of the two factors in this product.

Efforts to maintain nonperiodic grids for grating lobe reduction have centered mostly about use of circularly disposed arrays with an aperiodic arrangement of elements of one or several sizes.

An example is the array investigated by Patton.[111] This structure, shown schematically in Figure 18, consists of a circular array of dipole subarrays arranged in an aperiodic fashion. This array is locally periodic, and does have vestigal grating lobes, but these are considerably suppressed for a large array. Patton describes a 30-ft diameter array and a 10-ft diameter array at C-band. The 30-ft array consists of one thousand elements that scan a 0.36^o beam approximately 5^o with an element use factor of 1.3. The system has high average sidelobes at its maximum scan and losses which add to 5.94 dB for the 10 ft model and a projected 4.21 dB for the 30 ft array. The transmission line interconnections may also make an X-band design somewhat less practical. Peak sidelobes were measured at the -15 dB level for the 10-ft diameter array, and are projected at -20.9 dB for the 30 ft array, but the item of primary importance is the achievement of this extremely low element use factor and the low generalized f/D ratio achievable with aperiodic array technology.

A similar antenna, but using unequal size elements has recently been described by Manwarren and Minuti.[112] This antenna has been designed to provide a 1^o pencil beam at 1300 MHz to scan a conical sector with 8^o half angle with 20 dB grating lobes. An S-band model has also been configured. The antenna consists

111. Patton, W.T. (1972) Limited scan arrays, in phased array antennas, Proc. of the 1970 Phased Array Antenna Symposium, edited by A.A. Oliner and G.H. Knittel, Artech House, Inc., MA, 332-343.

112. Manwarren, T.A., and Minuti, A.R. (1974) Zoom Feed Technique Study, RADC-TR-74-56, Final Technical Report.

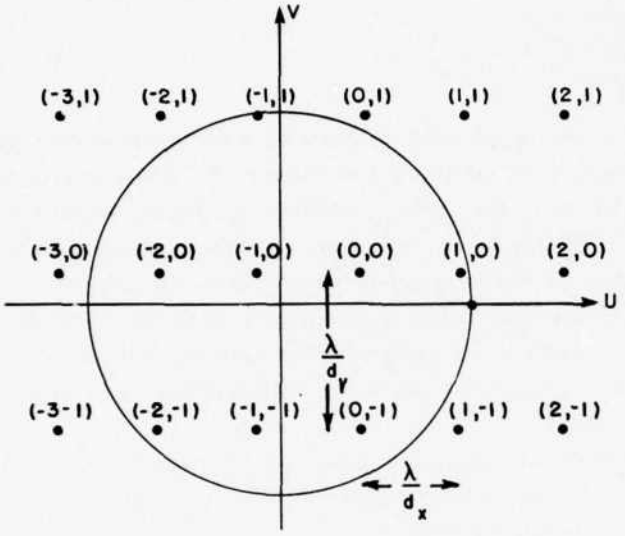

Figure 16. Periodic Array Grating Lobe Lattice

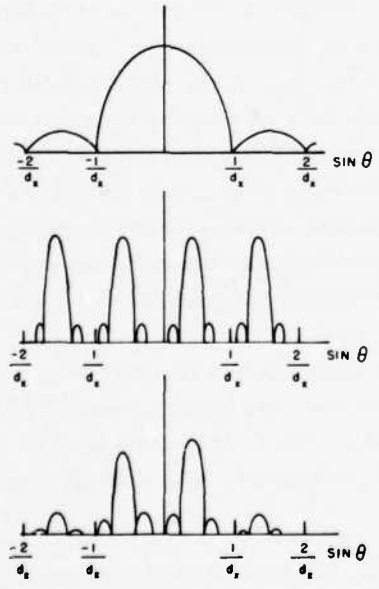

Figure 17. The Array Pattern, Element Factor Product

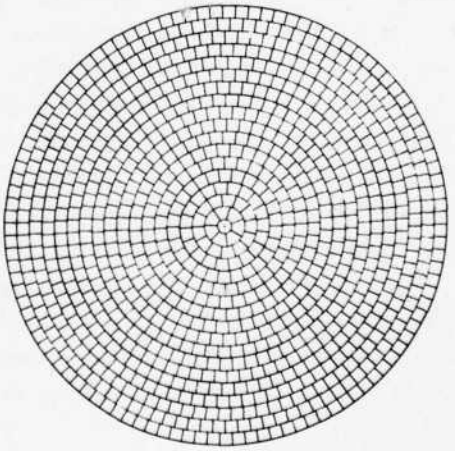

Figure 18. Element Location Diagram for the REST Array: A Technique for Limited Sector Coverage

of 412 elements of three different sizes to make up the array surface. The elements are arranged in concentric rings to produce a pseudorandom grid as done in the Rest program, but with additional randomness introduced by the unequal size elements. Computed patterns show graceful gain degradation with scan and grating lobes at the desired levels.

A recent effort at RADC/ET has revealed that relatively large aperture horns can be used as elements of a limited scan array if the higher order mode amplitude is actively controlled.[113] The technique is called multimode scanning and consists of choosing odd mode amplitudes and phases so that the combined element radiation pattern from any horn has a zero at the angle of the grating lobe nearest to broadside.

The required odd mode amplitude and phases are obtained from a knowledge of the element patterns for even and odd modes. An array for E-plane scan has its field pattern given by: (for $(\Delta_n) = 0$)

$$E(u, v) = E_x(u) \sum_{n=1}^{N_y} I_n^E \, e_y(v) \, e^{j\frac{2\pi}{\lambda}(v-v_o)nd_y} \tag{48}$$

element pattern $e_y(v)$ is zero at the grating lobe positions $v_q = \pm q\lambda/d_y$ corresponding to broadside main beam position for a uniformally illuminated element. The growth of the $q = -1$ grating lobe as a function of scan can be nearly eliminated by actively controlling $e_y(v)$ to place a zero at this grating lobe for all scan angles. In a waveguide circuit such control is accomplished by exciting the aperture with two modes (the LSE_{10} and LSE_{11}) instead of just the dominant LSE_{10} mode, so that $e_y(v)$ becomes the sum of two terms, with a zero at $v = v_o - \lambda/d_y = v_{-1}$. Choosing the ratio of odd mode to even mode as R_{11}, the combined element pattern is:

$$e_y(v) = e_{yo}(v) + R_{11} \, e_{y1}(v) \tag{49}$$

choosing $e_y(v)$ to be zero at the position of the $q = -1$ grating lobe one obtains for R_{11}

$$R_{11} = \frac{-e_{yo}(v_{-1})}{e_{y1}(v_{-1})} \quad . \tag{50}$$

113. Mailloux, R.J., and Forbes, G.R. (1973) An array technique with grating-lobe suppression for limited-scan application, IEEE Trans. AP-21(No. 5): 597-602.

Since the various waveguide modes have constant phase aperture distribution e_{yo} is a real function and e_{y1} is pure imaginary, so the R_{11} is pure imaginary and increases with scan in order to maintain the null position coincident with the center of the q = -1 grating lobe. The relative odd mode phase is thus fixed at $\pm 90^{o}$ with respect to the even mode phase depending upon the sense of the scan angle. The allowable element spacing for E-plane horns is

$$(d_y/\lambda) \sin \theta_{max} = 0.6 \quad . \tag{51}$$

The laboratory model shown in Figure 19 is an array designed for E-plane scan ($\pm 12^{o}$).

Figure 20 shows the E-plane pattern for the array phased at broadside and the elements excited with the central four at uniform amplitude, the second element in from each end of the array at -3 dB amplitude, and the outer elements at -6 dB amplitude. This taper should have first sidelobes at about -19 dB, but due to phase errors the level is approximately -17 dB. The grating lobes at $\pm 19^{o}$ (-16 dB) and $\pm 40^{o}$ (-26 dB) can be reduced by using a dielectric lens in each horn.

Figure 21 shows two cases at the maximum scan angle $\pm 12^{o}$. The dashed curve is the horn array radiation pattern without odd modes and shows that the main beam gain is reduced more than 5 dB with respect to the broadside array and the grating lobe at -7^{o} is larger than the main beam by 1.8 dB. Other grating lobes are at tolerable levels. The solid curve shows that when the element is excited by two modes the offending grating lobe is reduced to approximately the -20 dB level, and the main beam increased to -1.2 dB with respect to broadside because the new element pattern has its peak tilted toward the main beam. The second grating lobe (q = -2) is approximately the -12 dB level.

Conventional aperture tapering procedures can be used to reduce near sidelobe levels to -30 dB or less. The nulled grating lobe is suppressed 20 to 25 dB at center frequency for a small array (8 elements), but substantially more for larger arrays. Residual grating lobes at wider angles are unaffected by array tapering and remain the major limitation of the technique.

Full two-dimensional scanning requires the suppression of three grating lobes, however, and so a total of three higher order modes must be controlled as a function of scan. The dominant grating lobes to be cancelled are those nearest broadside (p, q) = (-1, 0), (-1, -1), (0-1) for general scan angles, and this control is achieved using four phase shifters for each multimode horn to form an element pattern that is separable in u-v space and positions the three nulls properly. In practice, it is also sometimes appropriate to narrow the horn H-plane patterns by

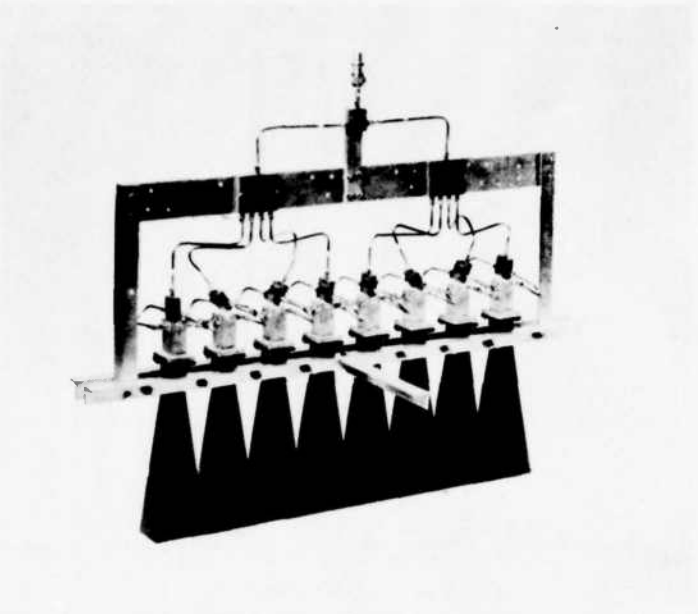

Figure 19. Laboratory Model Multimode Scanning Array

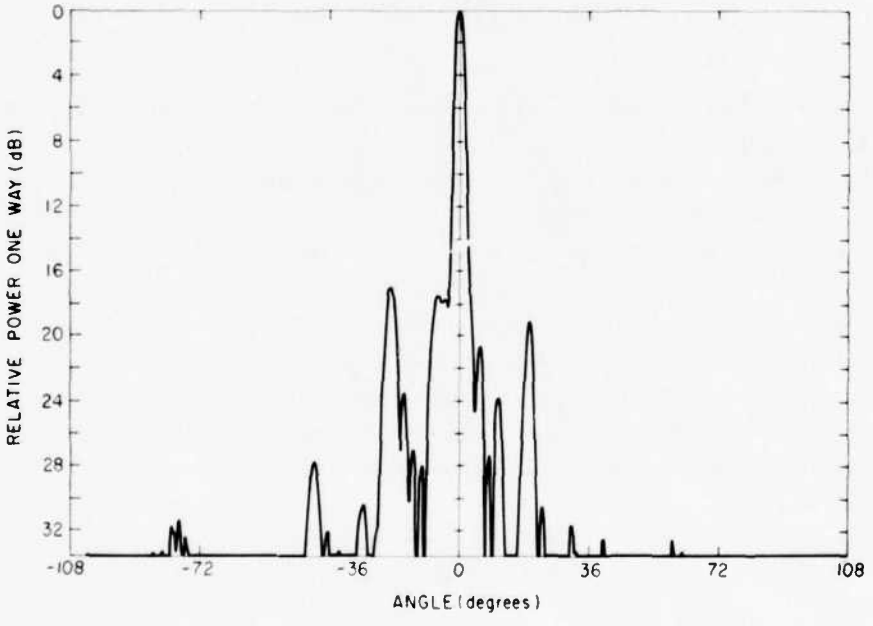

Figure 20. Broadside Pattern Data (Eight Element Array)

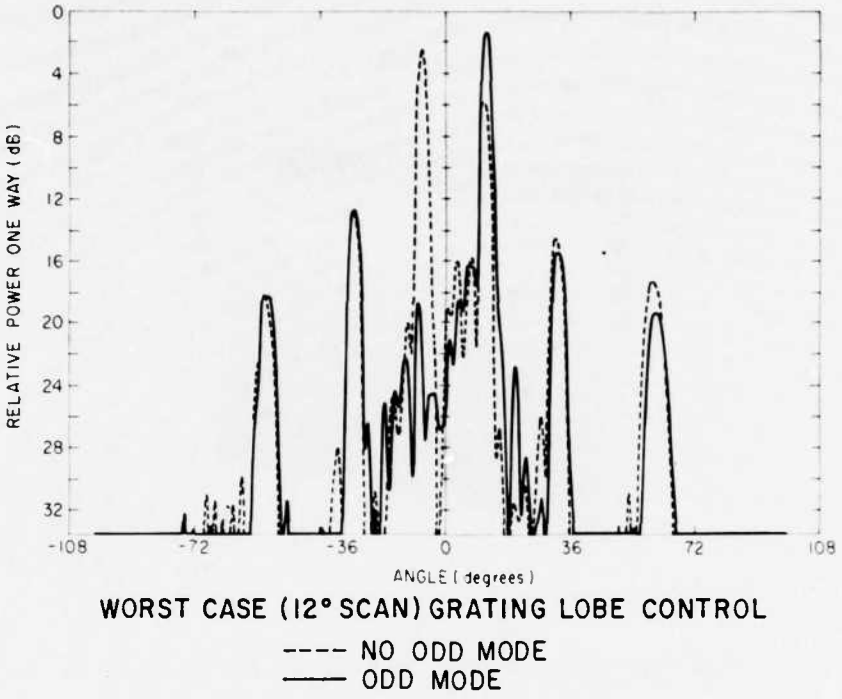

Figure 21. End of Scan Pattern Data (Eight Element Array)

dielectrically loading them.[114] This correction is added to minimize broadside H-plane grating lobes.

Bandwidth and far sidelobe levels are the most important limitations of the technique. Good performance has been achieved over narrow bandwidths (~3 percent), and bandwidths of up to 10 percent appear feasible. Far sidelobe (grating lobe levels) of -20 dB can now be obtained using various aperiodic row displacements [Δ_n] and spatial filtering combinations as will be described later, but it is unlikely that sidelobes can be reduced much below that level. The main advantages of the technique in comparison with most of the reflector or lens schemes are the availability of extremely low near sidelobes, the naturally high aperture efficiency and small antenna volume for any desired gain, and the use of row-column steering commands.

A final limited-scan antenna type is described as having "overlapped subarrays." This concept is an outgrowth of the realization that the ideal element for a limited

114. Tsandoulas, G.N., and Fitzgerald, W.D. (1972) Aperture efficiency enhancement in dielectrically loaded horns, IEEE Trans. AP-20(No. 1) 69-74.

scan system would have a flat top and no sidelobes. An element pattern like that of Figure 22 would allow the beam to scan out to some maximum scan angle ($\sin \theta_m$) while suppressing all grating lobes as long as they did not occur within the range $-\sin \theta_m \leq \sin \theta \leq \sin \theta_m$. Since the grating lobes occur at positions given by Eq. (47), then for a very large array one can optimize the interelement spacing for a given maximum scan angle by choosing

$$(d_x/\lambda) \sin \theta_m = 0.5 \tag{52}$$

where d_x is the intersubarray spacing. This condition was derived earlier (Eq. 41) from the basis of satisfying the criteria given for minimizing the number of phase controls, but here it results from choosing the widest possible flat-topped subarray pattern consistent with good grating lobe suppression. In this case a large array with main beam at $\sin \theta = (0.5\lambda/d_x)$ for some arbitrarily small value will have its nearest grating lobe at $\sin \theta = -(0.5\lambda/d_x)$, and all grating lobes will be completely suppressed. Such an array is characterized as a limited scan design because it can take advantage of limitations imposed upon the scan sector in order to increase aperture size d_x/λ. In principle an array with $\sin \theta_m = 0.1$ can use a 5λ interelement spacing while for $\sin \theta_m = 0.05$, a 10λ spacing can be used. This size increases and associated reductions in the number of required phase controls for restricted coverage illustrate the goal of limited scan antenna designs.

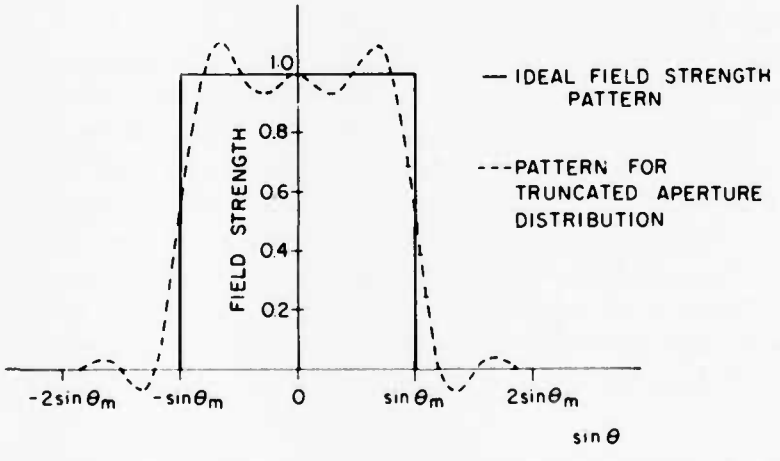

Figure 22. Ideal and Approximate Subarray Patterns for Overlapped Subarray

The aperture field corresponding to this far-field distribution is of the form:

$$i(x) = \frac{\sin\left(\frac{2\pi}{\lambda} x \sin\theta_m\right)}{\left(\frac{2\pi}{\lambda} x \sin\theta_m\right)} \tag{53}$$

where x is the distance measured from the center of the subarray. If the maximum ideal spacing $d_x/\lambda = (0.5/\sin\theta_m)$ is used, then this aperture distribution has zeros at $x = \pm nd_x$ excluding $n = 0$, and one must include a number of elements in order to reproduce the i(x) distribution faithfully. Thus, each phase shifter must feed a multiplicity of subarrays and the subarrays can be said to be overlapped. Obviously, the ideal aperture field can only be approximated; it must be truncated and then approximated by realizable distributions at each element. The dashed curve shown in Figure 22 shows the flat-topped subarray pattern achievable if the i(x) is truncated at $x = \pm 3d_x$. In this case, 20 dB grating lobe suppression can be obtained for scan out to the angle

$$(d_x/\lambda) \sin\theta_m = 0.43 \quad . \tag{54}$$

The required overlapped distribution implies the interconnection of a number of array elements and so is extremely difficult to fabricate in microwave circuitry. Consequently, the circuit approach has received only limited attention. Alternatively, space feed systems can quite naturally achieve overlapped subarray distributions that have proven very practical. These systems use feedthrough lenses or reflectors that can faithfully reproduce a substantial part of the f(x) distribution as compared with microwave circuit systems.

Examples of such schemes for producing optically overlapped subarrays includes the HIPSAF antenna[115] and the dual reflector-array design of Tang et al.[109] Figure 23 shows schematically that exciting two adjacent feed horns results in two overlapped aperture illuminations at the main reflector. These "subarray" aperture distributions have approximately (sin x)x fields and so have rectangular shaped radiation patterns as appropriate for good grating lobe suppression. Figure 24 shows a calculated and a measured pattern from the central subarray of the experimental reflector. Details of this extensive analytical and experimental study are included in the reference,[109] but in general the program demonstrated that such optical techniques can produce low sidelobe (<-20 dB)

115. Tang, R. (1972) Survey of time-delay beam steering techniques, in Phased Array Antennas, Proceedings of the 1970 Phased Array Antenna Symposium, Artech House Inc., MA, 254-270.

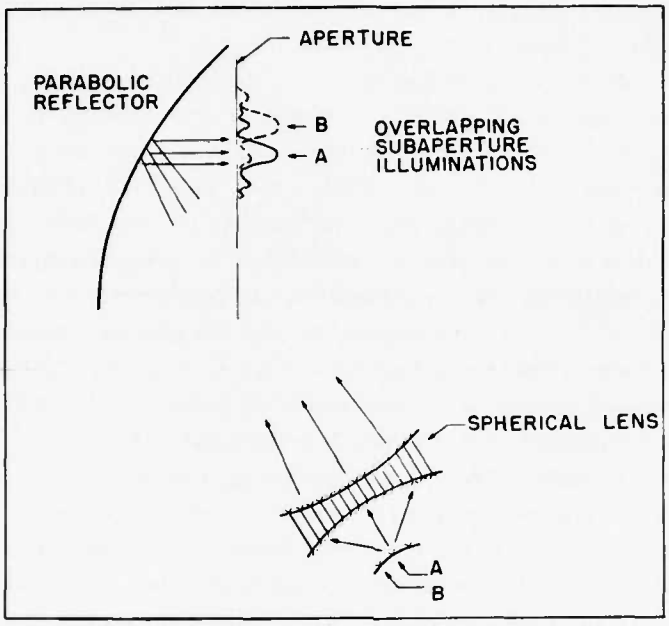

Figure 23. Aperture Illumination From Optically Overlapped Feed

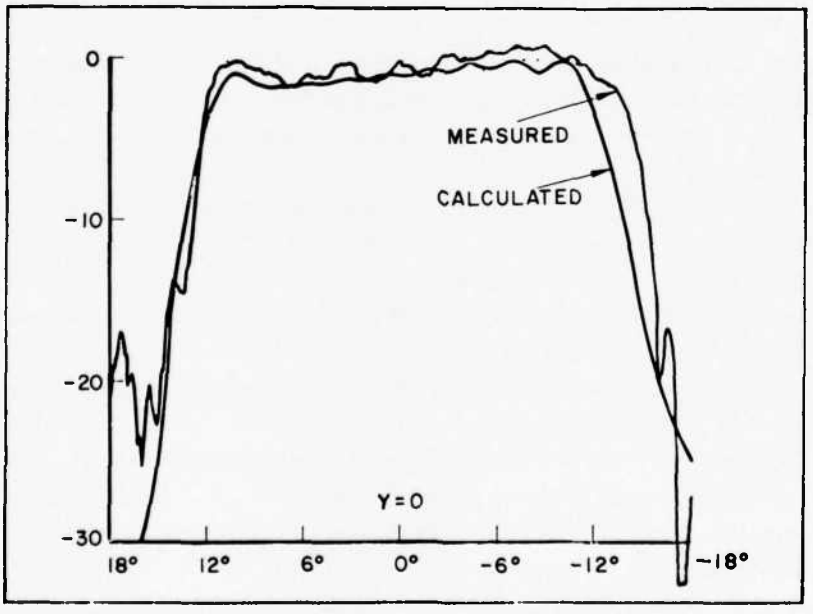

Figure 24. Subaperture Far Field Pattern for Central Subaperture

scanned patterns over limited spatial sectors using only about 1.4 times the theoretical minimum number of phase controls.

Apart from these configurations using quasioptical techniques, the ultimate in overlapped circuitry for low sidelobe arrays will, of necessity, be synthesized using constrained feed distribution networks. This is a new area of technology and there has been relatively little work in this area. Several studies of overlapped subarrays are reported by Tang, and modifications of these have recently been implemented for fire control radars. In addition the subarray distribution that produces an approximate flat topped pattern can be approximated by higher order mode distributions[116] in horn apertures, so that the element spacings can be made equal to the distance d between subarrays. This work is an outgrowth of studies on the active odd-mode control of element radiation patterns, but the developments in overlapped subarrays differ in concept, in means and in results from the multimode scanning technique. The study describes a passive interconnecting network to synthesize a flat topped, symmetric, subarray pattern, while the multimode scanning technique requires active control of odd-mode amplitude and achieves much greater scan per element (although slightly less per phase shifter).

The basic circuit allows an element size times scan angle product in the E-plane of approximately

$$(d_y/\lambda) \sin \theta_m = 0.33 \quad . \tag{55}$$

The largest array grating lobes are less than -16 dB for maximum scan. Circuits have been devised to provide similar overlapped behavior for two planes of scan, but there is not yet sufficient data to compare the relative advantage gained by using the second plane.

The discussion of limited scan arrays has dealt mainly with a description of methods devised to reduce array costs; and these methods form the basis of an evolving technology. The most significant change forthcoming in this area is the development of techniques for extremely low sidelobe control. These techniques will be aided by some established methods of sidelobe suppression (random element positions, and tunnel structures) and by the spatial filtering technique to be described later, but the basic antenna structures themselves must be substantially improved in order to achieve sidelobe levels between -35 and -45 dB. The only limited scan antenna with evidence showing that such sidelobe levels are achievable is the array-lens concept of Schell. These data are not yet published and consist at present of analytical calculations that neglect coupling and near field effects; but they confirm that the possibility of such extra-low sidelobe control exists.

116. Mailloux, R.J. (1974) An overlapped subarray for limited scan application, IEEE Trans. AP-22.

Other quasioptical approaches can conceivably produce extremely low sidelobes; in particular those schemes based upon overlapped subarraying approaches should produce very low sidelobe distributions, although not out to the scan limits given in this description.

None of the array techniques discussed here can produce patterns with such low sidelobes except through the use of spatial filtering; but techniques based upon constrained feed circuits for overlapped distributions can ultimately produce the lowest sidelobe limited scan systems. As yet there has been relatively little effort directed toward synthesizing such networks, and this remains an area where much work is needed.

3.4 Broadband and Multiple Frequency Arrays

Though considered together, broadband and multiple frequency arrays call for fundmentally different technology. Wideband arrays have one beam formed by a feed network and a set of phase shifters, but multiband technology has developed by interleaving relatively narrow band elements with different center frequencies, and with separate beamformers for each frequency.

The maximum theoretical bandwidth of linearly polarized rectangular waveguide phased arrays is about 60 percent.[117] Studies[118, 119] of such elements have indeed shown that these bandwidths can be achieved with low VSWR and wide scan coverage. Recent efforts sponsored by AFCRL (now RADC/ET) have developed double ridged waveguides[120] and novel stripline radiators,[121] see Figure 25, that can provide good performance over an octave bandwidth (67 percent). Arrays with circular polarization have much narrower bandwidths, with 25 percent seen as a reasonable outer limit.[122, 123]

---

117. Tsandoulas, G.N. (1972) Wideband limitations of waveguide arrays, Micro Microwave Journal 15(No. 9):49-56.

118. Chen, C.C. (1973) Broadband impedance matching of rectangular waveguide phased arrays, IEEE Trans. AP-21:298-302.

119. Laughlin, G.J., et al (1972) Very wide band phased array antenna, IEEE Trans. AP-20:699-704.

120. Chen, C.C. (1972) Octave band waveguide radiators for wide-angle scan phased arrays, IEEE AP-S Int. Symp. Record, 376-377.

121. Lewis, L.R., Fassett, M., and Hunt, J. (1974) A broadband stripline array element, IEEE AP-S Int. Symp. Record.

122. Chen, M.H., and Tsandoulas, G.N. (1973) Bandwidth properties of quadruple-ridged circular and square waveguide radiators, IEEE AP-S Int. Symp. Record, 391-394.

123. Tsandoulas, G.N., and Knittel, G.H. (1973) The analysis and design of dual-polarization square waveguide phased arrays, IEEE Trans. AP-21: 796-808.

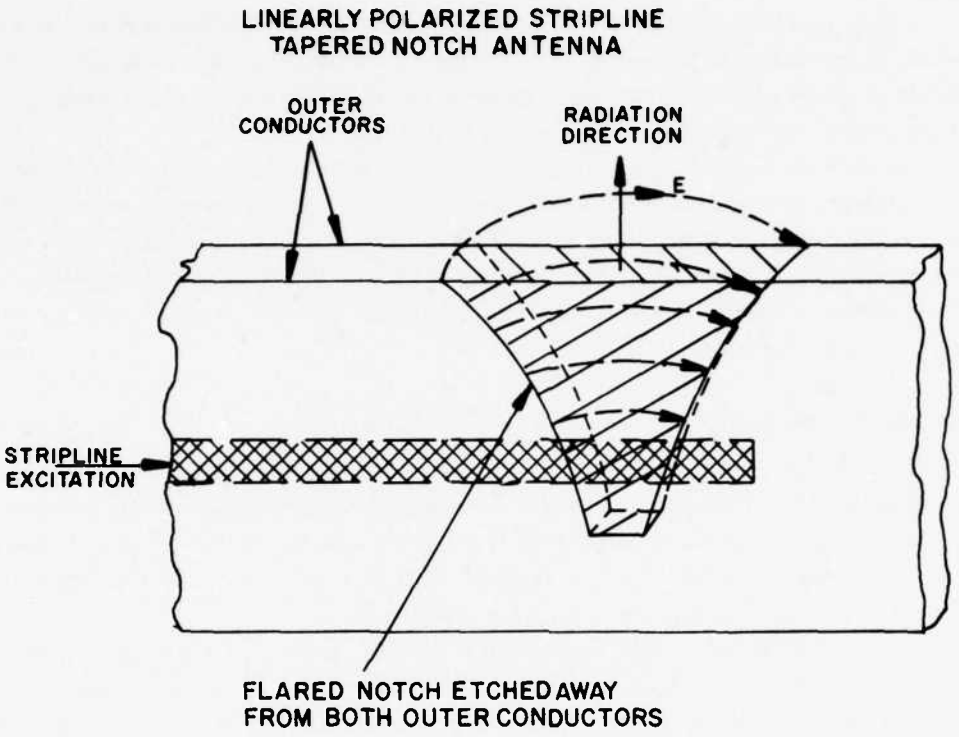

Figure 25. Wideband Stripline Flared Notch Element

Most of the development in dual band arrays has concerned interleaved arrays with ingenious brickwork patterns of various size elements,[124-127] with each frequency occupying a portion of the total aperture. A new RADC effort has led to the structure shown in Figure 26 as an array for two frequencies, one roughly double the other. An analysis of this structure was included in Section 2 for tutorial purposes. The advantages of this geometry are that both frequencies occupy the whole array aperture and that separate terminals are provided for independent steering of the two beams. Figure 27 shows the H-plane scan characteristics of this array at two distinct frequencies, and indicates that the array has good scan characteristics

124. Hsiao, J.K. (1971) Analysis of interleaved arrays of waveguide elements, IEEE Trans. AP-19:729-735.

125. Boyns, J.E., and Provencher, J.H. (1972) Experimental results of a multifrequency array antenna, IEEE Trans. AP-20:106-107.

126. Hsiao, J.K. (1972) Computer aided impedance matching of a interleaved waveguide phased array, IEEE Trans. AP-20:505-506.

127. Harper, W.H., et al (1972) NRL Report No. 7369, Naval Research Laboratory.

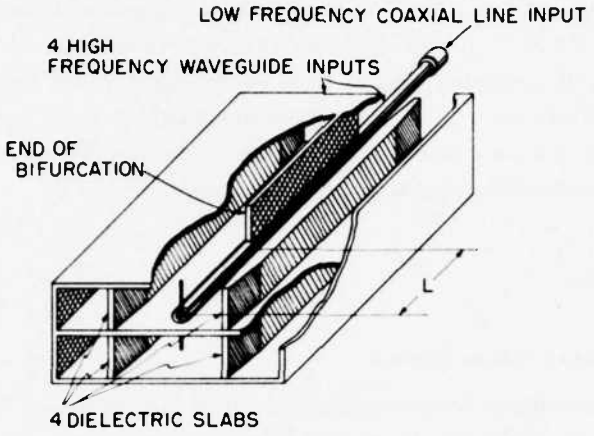

Figure 26. Dual Frequency Array Element

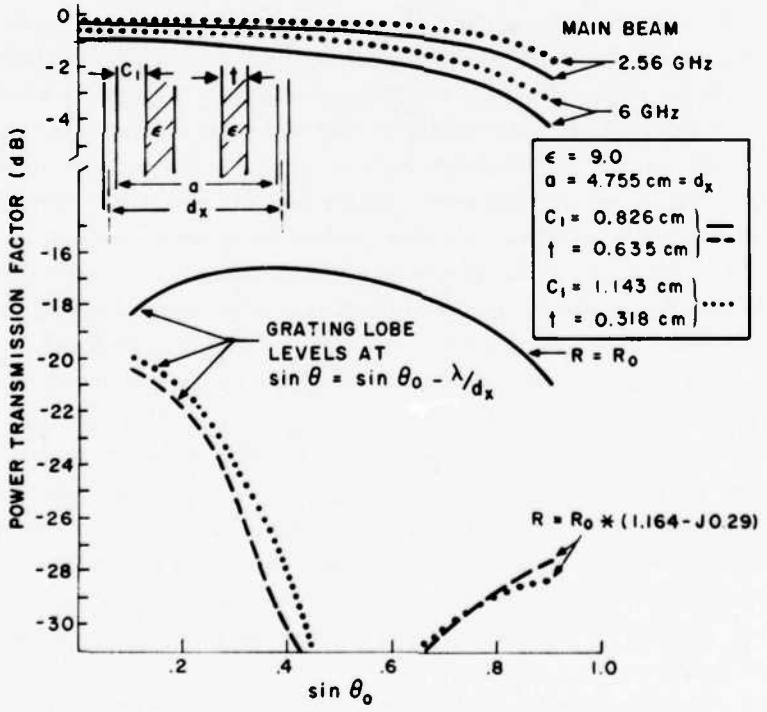

Figure 27. H-Plane Scanning Characteristics of Dual Frequency Array Element

with no blind spots within the scan sector at either frequency. The proper use of array matching techniques should improve these characteristics and so make the technique viable for high power radiation at both frequencies.

Other multiple frequency arrays have been proposed and developed for distinct applications, and this area of technology is evidently destined to play an expanding role in the future of array antennas as the number of aircraft terminals grows to meet the needs of satellite communication systems.

4. NEW TECHNOLOGY

4.1 New Technology as a Forcing Function

The techniques that have been discussed thus far represent major subject areas for research; the methods described represent present day solutions and may not correspond to ultimate solutions. The categorization "Special Purpose Arrays" thus defines an area that will be of major importance for many years. This section is addressed to a different kind of stimulus for array research; one based primarily upon the wide variety of transmission media. The thesis proposed is that the very rapid change in this technology can be a strong force that guides and propels a major part of the future of array antennas. The newer elements of technology include improved phase shifters, the emergence of microwave integrated circuit technology, and developments in stripline and microstrip transmission circuits. These new developments compliment existing array technology, but in addition they act as a stimulus to further advances in array techniques.

Figure 28 shows a waveguide phase shifter developed by Raytheon Company. The phase shifter developed by Raytheon itself is a three bit analog nonreciprocal device that handles 3.5 kW peak and has 1 dB loss. The photograph shows the driven circuit incorporated into the body of the phase shifter. Both ends of the phase shifter are matched to the environment they occupy. The front face is a linearly polarized C-band waveguide loaded with dielectric that has been matched to provide good properties over the design scan sector, while the back face is matched to optimize pickup from the space feed network. The main reason for showing this illustration is to indicate that indeed such scan matching has become practice; array behavior is calculated or measured in simulators, and phase shifters are incorporated to achieve compact units that plug into the array and can be conveniently replaced.

A second item of technology that further illustrates some of the above is shown in Figure 29. This laboratory prototype developed by Hughes Corporation is a 3-bit resistive gate diode phase shifter operating at S-band. Total loss is approximately 1.5 dB, the device can control 300 W of peak power with 5 W average. Its

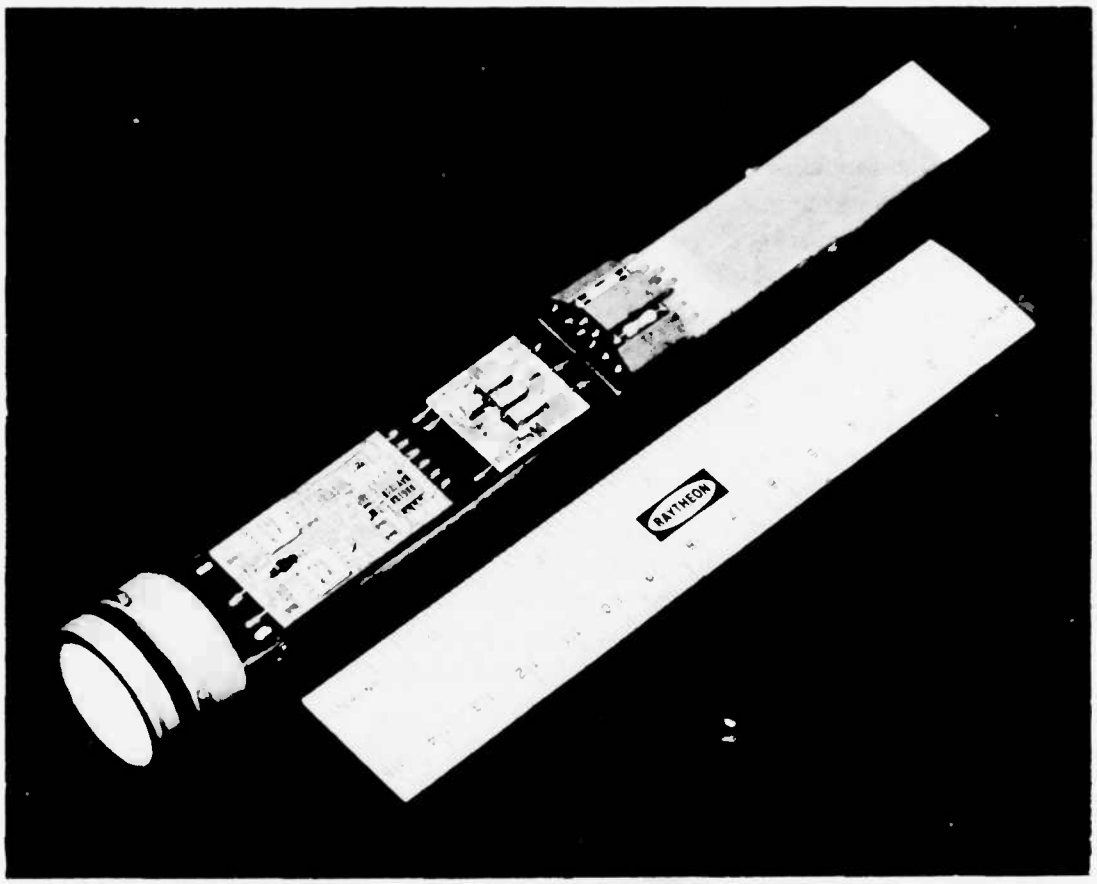

Figure 28. Exciter, Phase Shifter and Array Element

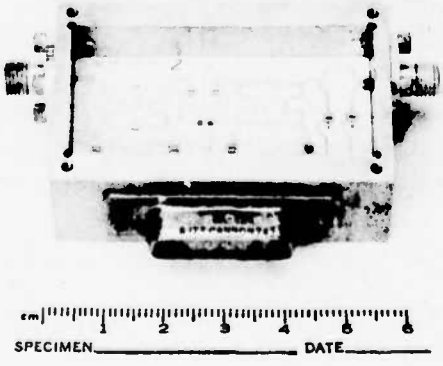

Figure 29. Resistive Gate Phase Shifter

size is approximately 1 in. by 1 in. by 2 in., and it switches in 10 μsec. The chief advantage claimed for this device is that the phase shifter does not require any forward bias current; the only bias current flowing through the device is a forward leakage current of several μA. Alternatively, the commonly used PIN diode phase shifters require 50-200 ma current at one volt forward and 100 volts at 1 μA reverse. Total power required for phase control per phase shifter and driver combination may thus be on the order of 0.3 to 0.6 W. The total power for a 2000 element array would thus be nearly 1 kW for the PIN diode array, but less than 0.2 W for a resistive gate diode array. This extremely low drive power requirement makes it possible to control the array steering from the beam steering computer without an additional driver and high power supply.

Apart from the obvious fact that diode phase shifters have come a long way, the second issue raised by this technology is that the emergence of microstrip transmission circuits has not carried through to microstrip scanned antennas. There have been a number of developments in microstrip devices with fixed beams,[128-131] but most of these early devices were not well suited to electronic scanning. Figure 30 shows a microstrip array of spiral elements developed by Raytheon Corporation. The array structure combines a corporate feed, power dividers, baluns, and phase shifting network on one printed circuit board.

To date, there are no comprehensive theoretical treatments of even single microstrip patch antennas. Nevertheless, the technology itself has advanced to such a degree that many of the larger corporations are developing numerous variations of the original designs, and the day of full scanned arrays is clearly very near. Research is needed in this important area in order to avoid some of the pitfalls that led to the problems of array blindness. Air Force applications for this type of lightweight, inexpensive, and conformable antenna array are many, and extend from man-pack designs to flush-mounted aircraft antennas. Studies of microstrip and the newer types of stripline antennas should be undertaken to assure that a valid technological base exists, and that its depth is sufficient to sustain the rapid technological growth that lies ahead.

A second technological area that has been a stimulus and could become a much more important factor in array design is the growth of active microwave integrated circuitry. Mixers, oscillators, and microwave amplifiers are now available

---

128. Munson, R.E. (1974) Conformal microstrip antennas and microstrip phased arrays, IEEE Trans. AP-22:74-78.

129. Howell, J.Q. (1975) Microstrip antennas, IEEE Trans. AP-23:90-93.

130. Kaloi, C. (1975) Asymmetrically Fed Electric Microstrip Dipole Antenna, TR-75-03, Naval Missile Center, Point Magee, CA.

131. Derneryd, A. (1976) Linearly polarized microstrip antennas, IEEE Trans. AP-24:846.

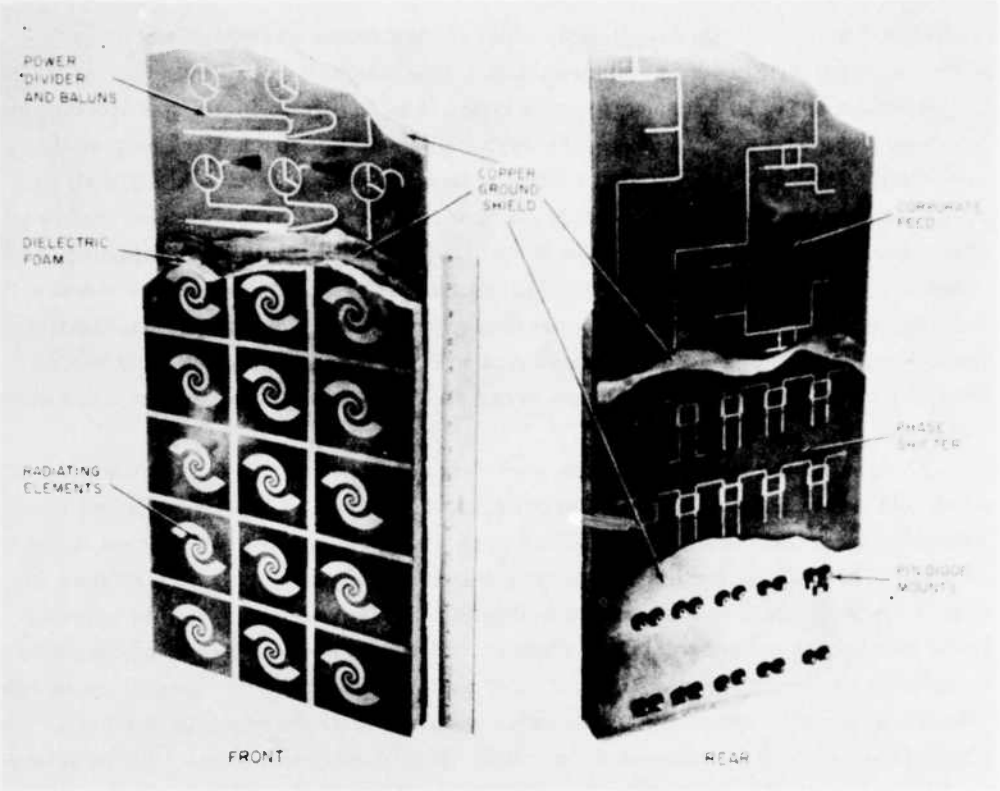

Figure 30. Microstrip Spiral Array Elements and Constrained Feed Network

throughout most of the microwave range, and are cost competitive for a growing number of array system applications.

At frequencies up to 4 GHz, transistors offer viable alternatives to the use of microwave tubes for many array applications. At higher frequencies, it is convenient to combine transistors with varactor multipliers. This procedure can, for example, yield 10 W at 4 GHz with better than 40 percent efficiency.[132] For frequencies up to X-band, IMPATT diodes can provide several watts of power and nearly 10 W is available from varactor multipliers. Gunn diodes can provide microwave signals at up to 70 GHz, but with relatively low signal levels at the high frequencies. A stimulating and timely survey of the current state of this art is given in the Microwave Journal.[132]

At present these devices tend to be too expensive for many applications, and the market is so small as to preclude the use of truly inexpensive production

132. Microwave Journal, Special Issue (1977) Solid state power, 20(No. 2).

methods. With time the use of solid state transmitters and receivers at each array element will become commonplace. This use will provide further stimulus for development of microstrip antenna types, and may also foster new developments in nonuniform array synthesis. The reasons for this additional concern is that such amplifiers are usually operated in a saturated mode, and it is difficult to amplitude weight the array elements as would be required for sidelobe suppression. The alternative is to allow uniform illumination and use nonuniform spacing for the purposes of tapering. This practice is not new; it is implemented in several military systems and numerous prototype design programs, but further exploration of these techniques for sidelobe suppression without undue complication of beam steering control requirements could bring about important advances in solid state radar arrays.

The continuing need to produce lower cost arrays has also led to the concept of an integrated subarray module approach. The array of Figure 30 is one early example of the technology required for such an approach, but the concept could be carried substantially further. Studies presently being undertaken by Hughes Aircraft Company are directed toward advancing such technology. In this approach a large number of radiators, phase shifters and a feed network are combined into an integrated subarray module which is used as the basic building block of an antenna. These components are combined on one common substrate of a high dielectric constant material such as alumina using thick film printing techniques. This printing technique can produce not only the conductor pattern of the circuits, but also the microwave capacitors and resistors as well. Radiators such as metallic discs are attached to the other side of the substrate (the ground plane side of the phase shifter circuit). This approach eliminates most of the interconnections such as coaxial cables and connectors, thereby reducing manufacturing and assembly labor as well as improving reliability. Radio frequency (rf) testing is performed at the subarray module level instead of the individual component level, hence, minimizing the testing cost. The ultimate subarray would have a continuous scanning aperture, that is, the phase shift across the radiating aperture is varied continuously for beam scanning. For example, a ferrite slab can be used as a radiating aperture. The index of refraction across the ferrite slab can be varied continuously by external magnetization for beam scanning. Preliminary results with a scanned aperture of this type have been demonstrated at Lincoln Laboratory.[133]

This description brings us to a limiting case, but emphasizes one of the main issues raised earlier. Array elements of the future may be very different from the waveguides and dipoles of the present. This technology must be supported by the

133. Stern, E., and Tsandoulas, G.N. (1975) Ferroscan: Toward continuous-aperture scanning, IEEE Trans. AP-23(No. 1):15-20.

same level of intense research activity that was necessary during the 60's because mistakes will be even more costly in the future.

4.2 Radomes, Polarizers, and Spatial Filters

4.2.1 METALLIC GRID STRUCTURES FOR RADOMES, DICHROIC REFLECTORS AND POLARIZERS

The present state-of-the-art in dielectric radomes is summarized in Walton.[134] There is a growing use of metallic gratings for radomes, polarizers, dichroic subreflectors, and, now possibly for spatial filters. These devices represent an area of research that is strongly influenced by, and can itself influence, phased array research.

The survey by Wait[135] compares various theories of wire grid and mesh structures that are the basis of this new technology. Much of the basic analysis was performed in the interest of developing improved ground plane surfaces and not for radomes or polarizers. Studies of artificial dielectrics as summarized by Collin[136, 137] are also directly applicable to the radome problem, as are the work of Kieburtz and Ishimaru,[138] Chen,[139] Pelton and Monk,[140] and the report by Luebbers,[141] which includes an extensive bibliography and presents a cataloging of the various periodic slot array geometries analyzed using modal matching techniques. There appear to be only several references that describe multiple layers of metallic gratings, and these are restricted to identical gratings.[142]

Apart from these analytical concerns, there has emerged an entirely new area of technology that offers metallic grid radomes or combinations of dielectric layers and metallic grids. The structures have been shown to have satisfactory wide-angle

---

134. Walton, J.D., editor (1970) Radome Engineering Handbook, Georgia Tech.

135. Wait, J.R. (1976) Theories of scattering from wire grid and mesh structures, Proc. of National Conference on Electromagnetic Scattering, University of Illinois.

136. Collin, R.E. (1955) Theory and design of wideband multisection quarter-wave transformers, Proc. IRE 43(No. 2):179-185.

137. Collin, R.E. (1960) Field Theory of Guided Waves, McGraw-Hill, 79-93.

138. Kieburtz, R.B., and Ishimaru, A. (1962) Aperture fields of an array of rectangular apertures, IRE Trans. AP-9:663-671.

139. Chen, C.C. (1971) Diffraction of electromagnetic waves by a conducting screen perforated periodically with circular holes, IEEE Trans. MTT-19 (No. 5):475-481.

140. Pelton, E.L., and Monk, B.A. (1974) A streamlined metallic radome, IEEE Trans. AP-22(No. 6):799-804.

141. Luebbers, R.J. (1976) Analysis of Various Periodic Slot Array Geometries Using Modal Matching, Report AFAL-TR-75-119, Ohio State University.

142. Monk, B.A., et al (1974) Transmission through a two layer array of loaded slots, IEEE Trans. AP-22:804-809.

transmission characteristics over moderate frequency ranges, and to incorporate the advantages of rigid, lightweight metallic structures with the desired electromagnetic qualities. A logical extension of the radome studies, the use of such grids for dichroic subreflectors has become common in recent years. Although there appears to be no single reference that summarizes this work, the references given in the Luebbers[141] report serve as a good introduction to the subject.

The related subject of wave polarizers for use with reflectors or array antennas is described in Young et al,[143] and Lerner.[144]

4.2.2 SPATIAL FILTERS FOR SIDELOBE SUPPRESSION

Low antenna sidelobe levels are a desirable attribute of ECM-resistant radar and communications systems. For many applications, one of the best ECCM features is a sidelobe level substantially below the range that is common to current systems. In order to reduce the vulnerability of existing systems that do not have very low sidelobes, it is often necessary to completely redesign the antenna. However, a new technology has been developed to provide an option that in certain cases can upgrade the ECCM capability of a radar or communications system without requiring antenna replacement. This technology is called spatial filtering.

Spatial filters are structures that are placed in front of an existing antenna to provide minimally attenuated transmission in the angular region near the main beam, while suppressing radiation in other directions. They consist of several parallel layers of uniform dielectric or metallic gratings with reflection coefficients of the layers and interlayer spacings chosen to produce the desired angular filter characteristic. Tradeoffs can be made among the frequency bandwidth, angular range of transmission, and filter characteristics by varying the physical parameters of the filter.

To date, only one example of a microwave spatial filter is found in the literature.[145] This filter was designed using dielectric layers and synthesized to have Chebyshev characteristics in space.

The principles of layered dielectric frequency domain filters are well established,[146] and insofar as possible the techniques for analysis and synthesis have been extended to the spatial domain. The fundamental difference between synthesis

---

143. Young, L., Robinson, L., and Hacking, C. (1973) Meanders-line polarizer, IEEE Trans. AP-21:376-378.

144. Lerner, D. S. (1965) A wave polarization converters for circular polarization, IEEE Trans. AP-13:3-7.

145. Mailloux, R.J. (1976) Synthesis of spatial filters with Chebyshev characteristics, IEEE Trans. Antennas and Propagation AP-24(No. 2)174-181.

146. Cohn, S. B. (1955) Optimum design of stepped transmission-line transformers, IRE Trans. MTT MTT-3(No. 2)16-21.

in the frequency domain and in the spatial domain, arises because the transmission coefficients of layers that have a high dielectric constant are strongly frequency dependent but relatively invariant with the angle of incidence. If a wave from a medium having a low dielectric constant is incident on a medium of high dielectric constant, then for any angle of incident the wave propagation direction in the latter is almost perpendicular to the interface.

This property necessitates a fundamental change in filter design from the frequency domain transformers synthesized by Collin[139] and others,[146-149] which consist of various dielectric layers sandwiched together. The spatial domain filters synthesized to date consist of quarter-wave sections of dielectric separated by half-wave or full-wave air spaces to produce a Chebyshev bandpass characteristic for the transmission response over an angular region.

Collin used the wave matrix formalism to derive convenient expressions for the transmission properties of layered impedance sections[137] and to describe the spatial properties of abutting dielectric layers.[136] The same formalism will be used here to derive properties of the stratefied dielectric filter. Consider the basic filter section shown in Figure 31. The incident and reflected waves in medium 1 are a_1 and b_1, respectively. The incident electric fields are assumed to be either parallel-polarized or perpendicularly polarized, with no cross-polarized components excited. The input-output parameters of the section are related by

$$\begin{pmatrix} a_1 \\ b_1 \end{pmatrix} = \begin{pmatrix} A_{11} & A_{12} \\ A_{21} & A_{22} \end{pmatrix} \begin{pmatrix} a_2 \\ b_2 \end{pmatrix} \quad . \tag{56}$$

The parameters A_{mn} can be related in terms of the conventional scattering matrix. The wave matrix of a cascade of networks is the product of the wave matrices of each network. A parameter of particular importance is

$$A_{11} = \left. \frac{a_1}{a_2} \right|_{b_2=0} \tag{57}$$

147. Riblet, H.J. (1957) General synthesis of quarter-wave impedance transformers, IRE Trans. MTT MTT-5(No. 1)36-43.

148. Young, L. (1959) Tables for cascaded homogeneous quarter-wave transformers, IRE Trans. MTT MTT-7(No. 2)233-244.

149. Young, L. (1962) Stepped-impedance transformers and filter prototypes, IRE Trans. MTT MTT-10(No. 5):339-359.

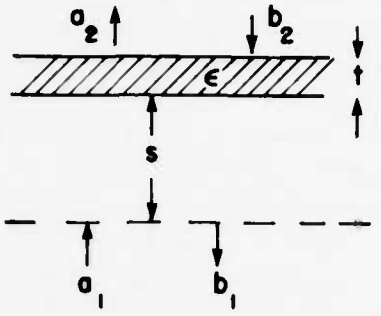

Figure 31. Spatial Filter Element

which is the inverse of the filter transmission coefficient. For the case of near-broadside incidence on a quarter-wave dielectric slab and air space of width S, the wave matrix is approximately

$$[A] = \begin{pmatrix} A_{11} & A_{12} \\ A_{21} & A_{22} \end{pmatrix} = \frac{1}{S_{12}} \begin{pmatrix} e^{jk_z S} & -S_{11} e^{jk_z S} \\ S_{11} e^{-jk_z S} & -e^{-jk_z S} \end{pmatrix} \tag{59}$$

where

$$S_{11} = \frac{\epsilon - 1}{\epsilon + 1} \quad , \quad S_{12} = \frac{-2j\sqrt{\epsilon}}{\epsilon + 1} \quad \text{and} \quad k_z = k_o \cos\theta \quad .$$

The angle θ is the polar angle from broadside in air.

The wave matrix of a filter comprised of a number of such sections is obtained by multiplying in sequential order the matrices of the sections, as

$$[A]_{\text{filter}} = \prod_{n=1}^{N} [A(S_n, \epsilon_n)] \quad . \tag{60}$$

This procedure is used with exact, angle dependent values of S_{11} and S_{12} to derive the filter properties for parallel and perpendicular polarizations and arbitrary angles of incidence,[145] but the synthesis procedure is accomplished using the broadside values of these parameters.

The procedure for filter synthesis depends on the properties of the polynomial expression for the power loss ratio, defined by Collin[137] as the power ratio associated with the inverse of the filter transmission coefficient:

$$P = A_{11}A_{11}^{*} \quad . \tag{61}$$

The power loss ratio of a filter consisting of quarter-wave sections of transmission line can be expressed as an even polynomial of degree 2n, where n is the number of sections in the filter. Synthesis is accomplished by equating the power loss ratio of the n layer filter equal to unity plus the square of a Chebyshev polynomial or order n.

The difference between the design for spatial filters and the work of Collin and others is the inclusion of the air spaces S_j between the dielectric layers. The electrical path length through the dielectric and the air-dielectric interface characteristics do not vary appreciably with the angle of incidence. It is the variation with angle of the paths through the air spaces that causes the filter properties.

A representative result of the synthesis procedure is shown in Figure 32. The filter consists of four layers with an interlayer separation of 0.5λ. The pass band extends to $\pm 11.5^{\circ}$ from broadside. The two inner layers of dielectric have a permittivity of $\epsilon_2 = 15.14$, while the outer dielectric layers have an $\epsilon_1 = 3.08$. The transmission characteristics for this filter have been calculated using the accurate formulation of the wave matrix, and the results are shown in Figures 33a and 33b. The filter reflection for the transmitted polarization and the cross-polarization are given. The u-axis ($u = \sin\theta\cos\phi$) is the H-plane, while the v-axis ($v = \sin\theta\sin\phi$) is the E-plane.

A four-section dielectric layer statial filter has been constructed. The filter consists of two outer layers of $\epsilon = 3$ dielectric and two inner layers of $\epsilon = 15$ dielectric material, each layer having a thickness of a quarter-wavelength in the material

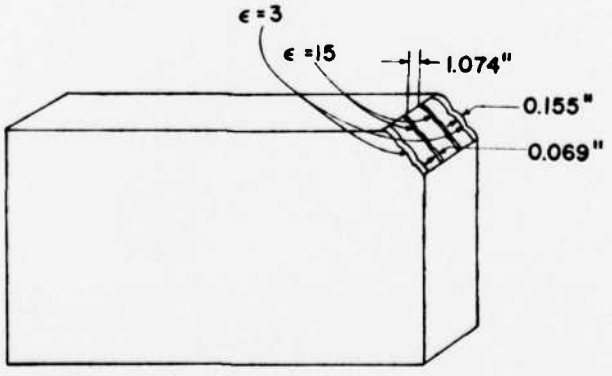

Figure 32. Experimental Model Spatial Filter

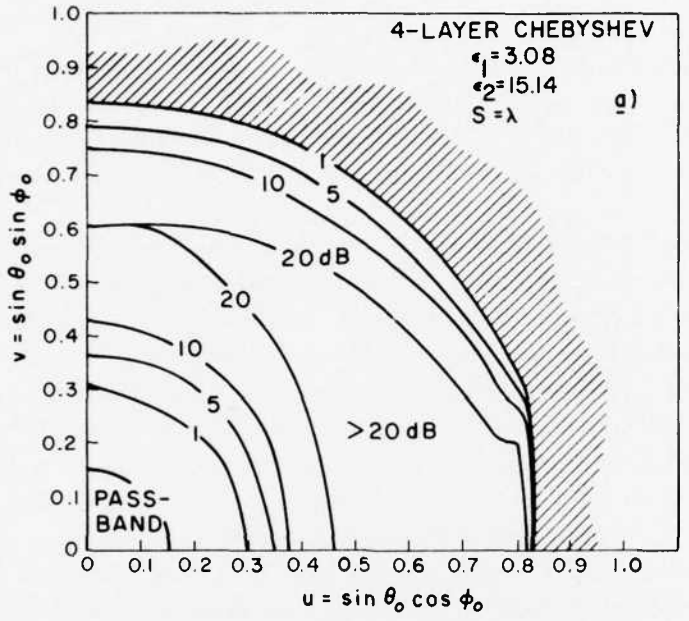

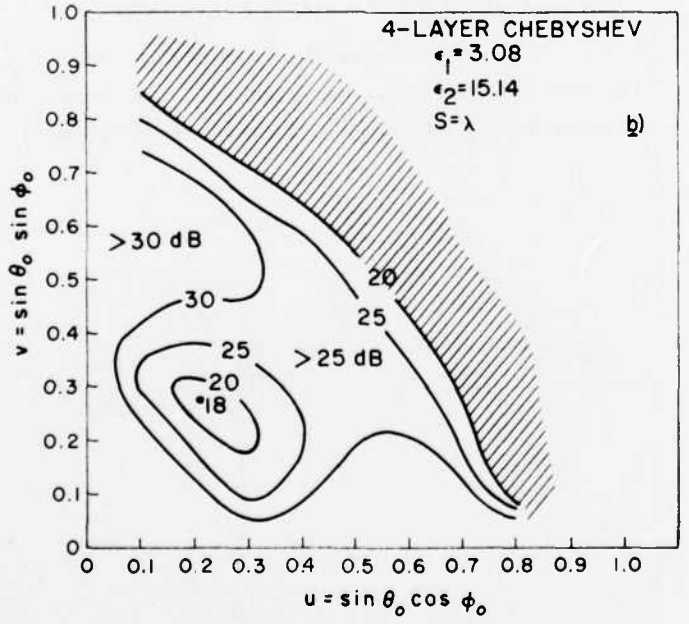

Figure 33. Characteristics of Experimental Filter

at 11 GHz. The spacing between layers is a free-space wavelength at 11 GHz. Each layer is approximately 25 × 75 cm in planar extent, and styrofoam is used between layers for stability.

Preliminary tests of this filter have been made using an array source. In Figure 34 are shown the radiation patterns of the array alone and the array with the filter. This array has a set of grating lobes that can be easily distinguished. Note that the filter attenuated those lobes falling within the stopband of the filter, but did not attenuate the grating lobe at $\theta = 60^{\circ}$, which is within the second pass-band of the filter.

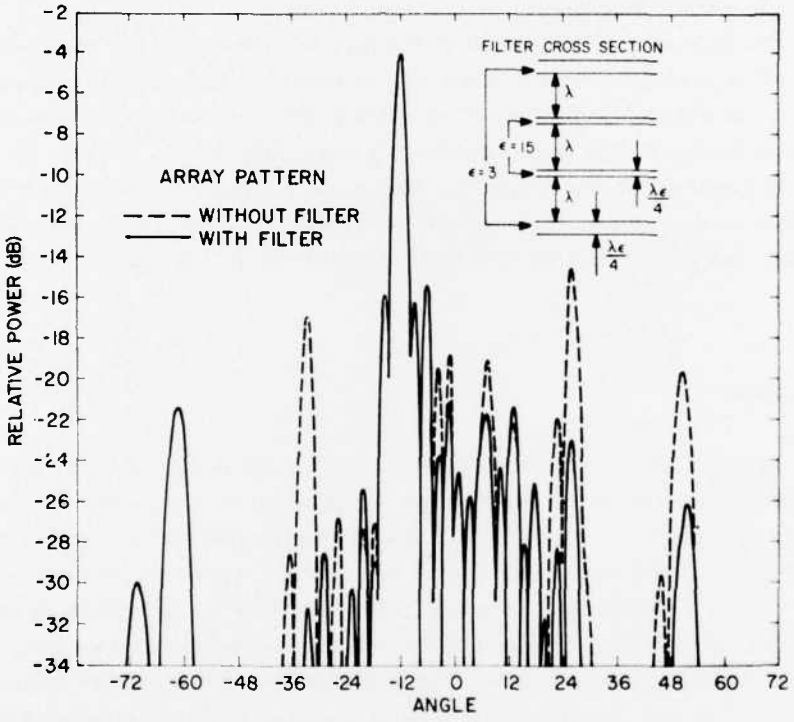

Figure 34. Grating Lobe Suppression Using the Experimental Filter

Although this preliminary study has been conducted using dielectric layers, the use of metallic grid structures has obvious advantages in both weight and cost as compared with dielectric layer filters. Under the assumption that mutual coupling can be neglected, the grid structures become shunt susceptances, and the

synthesis techniques described by Mathai and Young[150] can be used directly. To date there are no rigorous analytical results available that treat the problem of combining several unequal wire grids as required for spatial filter analysis.

Aside from the work described here, there is relatively little known about the characteristics of such spatial filters and their sidelobe suppression qualities. The example concerned the special case of a limited scan array with grating lobes, and even near the array the fields can be characterized by well defined plane waves. The array also has near fields that are characterized as nonpropagating waves (reactive fields), but these did not appear to have any significant influence on the experimental results. Remaining questions include what benefit the spatial filter can offer for far sidelobes that are due to random phase shifter errors or for sidelobes due to aperture blockage.

Preliminary results indicate that although the filter will obviously not improve the gain already reduced by blockage, it can reduce the resulting far sidelobe structure. In addition to studies of metallic grating structures for use as filter elements, there is thus a need for studying near-field effects such as the use of a filter near small diffrating obstacles, and in the presence of fields with pseudo-random phase variations. The potential advantages of the use of such filters is very great, but substantial research is required before this potential can be realized.

5. CONCLUSION

The purpose of this paper has been to provide some data that can be useful in predicting general trends in phased array technology over the next few years, and to identify pertinent research areas that will support this technology. The method chosen for developing these conclusions has been to describe some of the history of phased array research and then to show evidence of the acceleration pact of technological innovation. I believe this changing technology will uncover even more fundamental topics for array research than have been studied in prior years.

Stimulus for this growth is provided by military requirements for radar and communication; in particular by the need for rapid scanning, wide or multiple bandwidths, very low sidelobes, null steering and the constraints imposed by cost, size and in some cases the physical environment near the array. Born of this increased activity and these new stimuli is the "special purpose array;" a collection of many different array types that are each designed to satisfy only one set of

150. Mathai, G., Young, L., and Jones, E.M.T. (1964) Microwave Filters, Impedance Matching Networks and Coupling Structures, New York, McGraw-Hill, Chapter 9.

requirements, and are economically viable because they trade off other capability not related to any primary requirement. The growth of this collection of arrays has become so rapid as to provide a major focal point for activity in electromagnetic research. Added to this variety of new topics, there is antenna technology growing in response to the availability of solid state devices; this has caused development of a variety microstrip and stripline antennas which are quite fundamental new radiators with properties not yet fully investigated.

Finally, there is an area of growth that is occurring in response to uniquely military requirements, wideband antennas for ECM, multiple frequency antennas for satellite communication, extra low sidelobe and null steered arrays for ECCM radiation defense. Taken together, these forces have produced a major change in the direction of array research, and a need for increased research activity on a widening variety of topics within the general subject of array antennas.

References

1. Levine, H., and Schwinger, J. (1950, 1951) On the theory of electromagnetic wave diffraction by an aperture in an infinite plane conducting screen, Comm. on Pure and Applied Math 44:355-391.
2. Hallen, Erik (1938) Theoretical investigations into transmitting and receiving antennae, Nova Acta Regiae Soc. Sci. Upsaliensis (4) 11(No. 1).
3. King, R.W.P., and Harrison, C.W. (1969) Antennas and Waves, A Modern Approach, MIT Press, Cambridge, MA, (See Section 3.10).
4. Bouwkamp, C.J. (1954) Diffraction theory, Reports on Progress in Physics 17:35-100.
5. Mailloux, R.J. (1969) Radiation and near-field coupling between two collinear open-ended waveguides, IEEE Trans. AP-17(No. 1):49-55.
6. Lewin, L. (1970) On the inadequacy of discrete mode-matching techniques in some waveguide discontinuity problems, IEEE Trans. MTT-18(No. 7): 364-372.
7. Brouillion, L. (1953) Wave Propagation in Periodic Structures, Dover Publications, Inc.
8. Seckelmann, R. (1966) Propagation of TE modes in dielectric loaded waveguides, IEEE Trans. MTT-14:518-527.
9. Collin, R.E. (1960) Field Theory of Guided Waves, McGraw-Hill Book Co., Inc., New York.
10. Borgiotti, G.V. (1971) Edge effects in finite arrays of uniform slits on a groundplane, IEEE Trans. AP-19(No. 5):593-599.
11. Wasylkiwskyj, W. (1973) Mutual coupling effects in semiinfinite arrays, IEEE Trans. AP-21(No. 3):277-285.
12. Amitay, N., Galindo, V., and Wu, C.P. (1972) Theory and Analysis of Phased Array Antennas, New York, Wiley Interscience.
13. Carter, P.S., Jr. (1960) Mutual impedance effects in large beam scanning arrays, IRE Trans. AP-8:276-285.

14. King, R. W. P. (1956) The Theory of Linear Antennas, Harvard University Press, Cambridge, MA.

15. King, R. W. P., and Sandler, S. S. (1964) The theory of broadside arrays, and the theory of endfire arrays, IEEE Trans on Antennas and Propagation AP-12:269-275, 276-280.

16. Harrington, R. F. (1968) Field Computation by Moment Methods, McMillan Co., New York.

17. Harrington, R. F., and Mautz, J. R. (1967) Straight wires with arbitrary excitation and loading, IEEE Trans. AP-15(No. 4):502-515.

18. Lewin, L. (1951) Advanced Theory of Waveguides, Iliffe and Sons, Ltd., London, Chapter 6.

19. Cohen, M. H., Crowley, T. H., and Levis, C. A. (1951) The Aperture Admittance of a Rectangular Waveguide Radiating into a Half Space, (ATI-133707) Antenna Laboratory, Ohio State University, Research Foundation, Rept. 339-22.

20. Wheeler, G. W. (1950) Coupled Slot Antennas, Ph. D. Thesis, Harvard University, Cambridge, MA.

21. Levis, C. A. (1956) Variational Calculations of the Impedance Parameters of Coupled Antennas, Ohio State University Research Foundation, Rept. 667-16, Contract AF33(616)3353.

22. Galejs, J. (1965) Self and mutual admittances of waveguides radiating into plasma layers, Radio Sci, J. Res. NBS/USNC-URSI 69D(No. 2):179-189.

23. Richmond, J. H. (1961) A reaction theorem and it's applications to antenna impedance calculations, IRE Trans AP AP-8:515-520.

24. Lyon, J. A. M., Kalafus, R. M., Kwon, Y. K., Diegenis, C. J., Ibrahim, M. A. H., and Chen, C. C. (1966) Derivation of Aerospace Antenna Coupling – Factor Interference Predication Techniques, Tech. Rept. AFAL-TR-66-57, The University of Michigan, Radiation Laboratory.

25. Mailloux, R. J. (1969) Radiation and near-field coupling between two collinear open-ended waveguides, IEEE Trans on Antennas and Propagation AP-17: (No. 1):49-55.

26. Mailloux, R. J. (1969) First-order solutions for mutual coupling between waveguides which propagate two orthogonal modes, IEEE Trans. AP-17: 740-746.

27. Bailey, M. C. (1974) Finite planar array of circular waveguide apertures in flat conductor, IEEE Trans. AP-22:178-184.

28. Steyskal, H. (1974) Mutual coupling analysis of a finite planar waveguide array, IEEE Trans. AP-22:594-597.

29. Knittel, G. H., Hessel, A., and Oliner, A. A. (1968) Element pattern nulls in phased arrays and their relation to guided waves, Proc. IEEE 56:1822-1836.

30. Lechtreck, L. W. (1965) Cumulative coupling in antenna arrays, IEEE G-AP International Symposium Digest, 144-149.

31. Oliner, A. A., and Malech, R. G. (1966) Speculation on the role of surface waves, Microwave Scanning Antennas, Academic Press, N. Y., Vol. 2, 308-322.

32. Farrell, G. F., Jr., and Kuhn, D. H. (1966) Mutual coupling effects of triangular-grid arrays by modal analysis, IEEE Trans. AP-14:652-654.

33. Farrell, G.F., Jr., and Kuhn, D.H. (1968) Mutual coupling in infinite planar arrays of rectangular waveguide horns, IEEE Trans. AP-16:405-414.

34. Amitay, N., and Galindo, V. (1968) The analysis of circular waveguide phased arrays, Bell System Technical Journal, 1903-1932.

35. DuFort, E.C. (1968a) Design of corrugated plates for phased array matching, IEEE Trans. AP-16:37-46.

36. DuFort, E.C. (1968a) A design procedure for matching volumetrically scanned waveguide arrays, Proc. IEEE 56:1851-1860.

37. Mailloux, R.J. (1972) Surface waves and anomalous wave radiation nulls on phased arrays of TEM waveguides with fences, IEEE Trans. AP-20: 160-166.

38. Bates, R.H.T. (1965) Mode theory approach to arrays, IEEE Trans. and Propagation (Communieations) AP-13:321-322.

39. Byron, E.V., and Frank, J. (1968a) Lost beams from a dielectric covered phased-array aperture, IEEE Trans. AP-16:496-499.

40. Hannan, P.W. (1967) Discovery of an array surfaee wave in a simulator, IEEE Trans. AP-15:574-576.

41. Gregorwich, W.S., Hessel, A., Knittel, G.H., and Oliver, A.A. (1968) A waveguide simulator for the determination of a phased-array resonance, IEEE G-AP International Symposium Digest, 134-141.

42. Frazita, R.F. (1967) Surface-wave behavior of a phased array analyzed by the grating-lobe series, IEEE Trans. AP-15:823-824.

43. Parad, L.I. (1967) The input admittance to a slotted array with or without a dielectric sheet, IEEE Trans. (Communications) AP-15:302-304.

44. Galindo, V., and Wu, C.P. (1968) Dielectrie loaded and covered rectangular waveguide phased arrays, Bell System Teehnical Journal 47:93-116.

45. Wu, C.P., and Galindo, V. (1968) Surface wave effects on dielectric sheathed phased arrays of rectangular waveguides, Bell System Technical Journal 47:117-142.

46. Borgiotti, G.V. (1968) Modal analysis of periodic planar phased arrays of apertures, IEEE Proc. 56:1881-1892.

47. Allen, J.L. (1965) On surface-wave coupling between elements of large arrays, IEEE Trans. AP-13:638-639.

48. Lechtreck, L.W. (1968) Effeets of coupling aeeumulation in antenna arrays, IEEE Trans. AP-16:31-37.

49. Diamond, B.L. (1968) A generalized approach to the analysis of infinite planar array antennas, Proc IEEE 56(No. 11):1837-1851.

50. Oliner, A.A., and Malech, R.G. (1964) Speculation on the Role of Surface Waves, Microwave Scanning Antennas, Academic Press, N.Y., Vol. 2, 308-322.

51. Ehlenberger, A.G., Schwartzman, L., and Topper, L. (1968) Design criteria for linearly polarized waveguide arrays, IEEE Proc. 56(No. 11): 1861-1872.

52. Byron, E.V., and Frank, J. (1968b) On the eorrelation between wideband arrays and array simulators, IEEE Trans. (Communications) AP-16: 601-603.

53. Hessel, A., and Knittel, G. H. (1969) A loaded groundplane for the elimination of blindness in a phased-array antenna, IEEE G-AP International Symposium Digest, 163-169.

54. Knittel, G. H. (1970) The choice of unit-cell size for a waveguide phased array and its relation to the blindness phenomenon, Presented at Boston Chapter Antennas and Propagation Group Meeting.

55. Hessel, A., and Knittel, G. H. (1970) On the prediction of phased array resonances by extrapolation from simulator measurements, IEEE Trans. Antennas and Propagation (Communications) AP-18:121-123.

56. Mailloux, R. J. (1971) Blind Spot Occurrence in Phased Arrays – When to Expect It and How to Cure It, AFCRL-71-0428, Physical Sciences Research Papers, No. 462, Air Force Cambridge Research Laboratories.

57. Lee, S. W., and Jones, W. R. (1971) On the suppression of radiation nulls and broadband impedance matching of rectangular waveguide phased arrays, IEEE Trans. AP-19:41-51.

58. Lee, S. W. (1967) Radiation from the infinite aperiodic array of parallel-plate waveguides, IEEE Trans. AP-15(No. 5):598-606.

59. Harrington, R. F. (1967) Matrix methods for field problems, Proc. IEEE 55 (No. 2):136-149.

60. Amitay, N., Galindo, V., and Wu, C. P. (1972) Theory and Analysis of Phased Array Antennas, New York, Wiley-Interscience.

61. Harrington, R. F., and Mautz, J. R. (1975) A Generalized Network Formulation for Aperture Problems, AFCRL-TR-75-0589, Scientific Report No. 8, Contract F19628-73-C-0047.

62. Shelley, B. (1968) A matrix-fed circular array for continuous scanning, IEEE Proc. 56(No. 11):2016-2027.

63. Holley, A. E., et al (1974) An electronically scanned beacon antenna, IEEE Trans. AP-22:3-12.

64. Bogner, B. F. (1974) Circularly symmetric r. f. commutor for cylindrical phased arrays, IEEE Trans. AP-22:78-81.

65. Boyns, J. E., et al (1970) Step-scanned circular-array antenna, IEEE Trans. AP-18(No. 5):590-595.

66. Munger, A. D., et al (1974) Conical array studies, IEEE Trans. AP-22:35-43.

67. Hsiao, J. K., and Cha, A. G. (1974) Patterns and polarizations of simultaneously excited planar arrays on a conformal surface, IEEE Trans. AP-22: 81-84.

68. Gobert, W. B., and Young, R. F. H. (1974) A theory of antenna array conformal to surface revolution, IEEE Trans. AP-22:87-91.

69. Tsandoulas, G. S., and Willwerth, F. G. (1973) Mutual coupling in concave cylindrical arrays, Microwave Journal 16(No. 10):29-32.

70. Borgiotti, G. V., and Balzano, Q. (1970) Mutual coupling analysis of a conformal array of elements on a cylindrical surface, Trans. IEEE AP-18: 55-63.

71. Borgiotti, G. V., and Balzano, Q. (1972) Analysis of element pattern design of periodic array of circular apertures on conducting cylinders, IEEE Trans. AP-20:547-553.

72. Balzano, Q., and Dowling, T. B. (1974) Mutual coupling analysis of arrays of aperture on cones (Communications), IEEE Trans. AP-22:92-97.

73. Golden, K. E., et al (1974) Approximation techniques for the mutual admittance of slot antennas in metallic cones, IEEE Trans. AP-22:44-48.

74. J. Shapira, et al (1974) Ray analysis of conformal array antennas, IEEE Trans. AP-22:49-63.

75. Steyskal, H. (1974) Mutual coupling analysis of cylindrical and conical arrays, IEEE/AP-S Int. Symp. Record, 293-294.

76. Maune, J.J. (1972) An SHF airborne receiving antenna, Twenty Second Annual Symposium on USAF Antenna Research and Development.

77. Villeneuve, A.T., Behnke, M.C., and Kummer, W.H. (1973) Hemispherically Scanned Arrays, AFCRL-TR-74-0084, Contract No. F19628-72-C-0145, Scientific Report No. 2. Also, see 1974 International IEEE AP-S Symposium Digest, 363-366.

78. Balzano, Q., Lewis, L.R., and Siwiak, K. (1973) Analysis of Dielectric Slab-Covered Waveguide Arrays on Large Cylinders, AFCRL-TR-73-0587, Contract No. F19628-72-C-0202, Scientific Report No. 1.

79. Schwartzman, L., and Stangel, J. (1975) The dome antenna, Microwave Journal 18(No. 10):31-34.

80. Esposito, F.J., Schwartzman, L., and Stangel, J.J. (1975) The Dome Antenna-Experimental Implementation, URSI/USNC Meeting Digest 1975, June 3-5, Commission 6.

81. Ruze, J. (1952) Physical Limitations on Antennas, MIT Research Lab. Electronics Tech. Rept. 248.

82. Miller, C.J. (1964) Minimizing the effects of phase quantization errors in an electronically scanned array, Proc. 1964 Symp. Electronically Scanned Array Techniques and Applications, RADC-TDR-64-225, Vol. 1, 17-38, AD448421.

83. Allen, J.L. (1960, 1961) Some extensions of the theory of random error effects on array patterns, in J.L. Allen et al., Phased Array Radar Studies, Tech. Rept. No. 236, Lincoln Laboratory, M.I.T.

84. Elliott, R.S. (1958) Mechanical and electrical tolerances for two-dimensional scanning antenna arrays, IRE Trans. AP-6:114-120.

85. McIlvenna, J.F., and Drane, C.J. (1971) Maximum gain, mutual coupling and pattern control in array antennas, The Radio and Electronic Engineer, 41(No. 12):569-572.

86. McIlvenna, J., et al (1976) The Effects of Excitation Errors in Null Steering Antenna Arrays, RADC-TR-76-183, Rome Air Development Center.

87. Stangel, J.J. (1974) A basic theorem concerning the electronic scanning capabilities of antennas, URSI Commission VI, Spring Meeting.

88. Patton, W.T. (1972) Limited scan arrays, in Phased Array Antennas; Proc of the 1970 Phased Array Antenna Symposium, edited by A.A. Oliner and G.H. Knittel, Artech House, Inc., MA., 332-343.

89. Borgiotti, G. (1975) Design Criteria and Numerical Simulation of an Antenna System for One-Dimensional Limited Scan, AFCRL-TR-75-0616.

90. Silver, S., and Pao, C.S. (1944) Paraboloid Antenna Characteristics as a Function of Feed Tilt, MIT Radiation Lab., Cambridge, MA, Rep 479.

91. Ruze, J. (1965) Lateral feed displacement in a paraboloid, IEEE Trans. Antennas Propagation AP-13:660-665.

92. Sletten, C.J., et al (1958) Corrective line sources for paraboloids, IEEE Trans. AP-6(No. 3):239-251.

93. Collin, R.E., and Zucker, F.J. (1969) Antennas Theory, Part 2, McGraw-Hill Book Co., New York, Chapter 17.

94. Rusch, W.V.T., and Ludwig, A.C. (1973) Determination of the maximum scan-gain contours of a beam-scanning paraboloid and their relation to the pitzval surface, IEEE Trans. Antennas Propagation, AP-21:141-147.

95. Imbraile, W.A., et al (1974) Large lateral feed displacements in a parabolic reflector, IEEE Trans. AP-22(No. 6):742-745.

96. Rudge, A.W. (1969) Focal plane field distribution of parabolic reflectors, Electronics Letters 5:610-612.

97. Rudge, A.W., and Withers, M.J. (1971) New techniques for beam steering with fixed parabolic reflectors, Proc. IEEE 118(No. 7):857-863.

98. Rudge, A.W., and Withers, M.J. (1969) Beam-scanning primary feed for parabolic reflectors, Electronic Letters 5:39-41.

99. Rudge, A.W., and Davies, D.E.N. (1970) Electronically controllable primary feed for profile-error compensation of large parabolic reflectors, Proc. IEEE 117(No. 2):351-358.

100. Winter, C. (1968) Phase scanning experiments with two reflector antenna systems, Proc. IEEE 56(No. 11):1984-1999.

101. White, W.D., and DeSize, L.K. (1962) Scanning characteristics of two-reflector antenna systems, 1962 IRE International Conv. Record, Pt. 1, 44-70.

102. Tang, C.H. (1970) Application of limited scan design for the AGILTRAC-16 antenna, 20th Annual USAF Antenna Research and Development Symposium, University of Illinois.

103. Howell, J.M. (1974) Limited Scan Antennas, IEEE/AP-S International Symposium.

104. Schell, A.C. (1972) A Limited Sector Scanning Antennas, IEEE G-AP International Symposium.

105. McGahan, R. (1975) A Limited Scan Antenna Using a Microwave Lens and a Phased Array Feed, M.S. Thesis, MIT.

106. Fitzgerald, W.D. (1971) Limited Electronic Scanning with an Near Field Cassegrainian System, ESD-TR-71-271, Technical Report 484, Lincoln Laboratory.

107. Fitzgerald, W.D. (1971) Limited Electronic Scanning with an Offset-Feed Near-Field Gregorian System, ESD-TR-71-272, Technical Report 486, Lincoln Laboratory.

108. Miller, C.J., and Davis, D. (1972) LFOV Optimization Study, Final Report No. 77-0231, Westinghouse Defense and Electronic Systems Center, System Development Division, Baltimore, Md., ESD-TR-72-102.

109. Tang, C.H., and Winter, C.F. (1973) Study of the Use of a Phased Array to Achieve Pencil Beam over Limited Sector Scan, AFCRL-TR-73-0482, ER 73-4292, Raytheon Co., Final Report Contract F19628-72-C-0213.

110. Tang, E., et al (1975) Limited Scan Antenna Technique Study, Final Report, AFCRL-TR-75-0448, Contract No. F19628-73-C-0129.

111. Patton, W.T. (1972) Limited scan arrays, in phased array antennas, Proc. of the 1970 Phased Array Antenna Symposium, edited by A.A. Oliner and G.H. Knittel, Artech House, Inc., MA, 332-343.

112. Manwarren, T.A., and Minuti, A.R. (1974) Zoom Feed Technique Study, RADC-TR-74-56, Final Technical Report.

113. Mailloux, R.J., and Forbes, G.R. (1973) An array technique with grating-lobe suppression for limited-scan application, IEEE Trans. AP-21(No. 5): 597-602.

114. Tsandoulas, G.N., and Fitzgerald, W.D. (1972) Aperture efficiency enhancement in dielectrically loaded horns, IEEE Trans. AP-20(No. 1) 69-74.

115. Tang, R. (1972) Survey of time-delay beam steering techniques, in Phased Array Antennas, Proceedings of the 1970 Phased Array Antenna Symposium, Artech House Inc., MA, 254-270.

116. Mailloux, R.J. (1974) An overlapped subarray for limited scan application, IEEE Trans. AP-22.

117. Tsandoulas, G.N. (1972) Wideband limitations of waveguide arrays, Microwave Journal 15(No. 9):49-56.

118. Chen, C.C. (1973) Broadband impedance matching of rectangular waveguide phased arrays, IEEE Trans. AP-21:298-302.

119. Laughlin, G.J., et al (1972) Very wide band phased array antenna, IEEE Trans. AP-20:699-704.

120. Chen, C.C. (1972) Octave band waveguide radiators for wide-angle scan phased arrays, IEEE AP-S Int. Symp. Record, 376-377.

121. Lewis, L.R., Fassett, M., and Hunt, J. (1974) A broadband stripline array element, IEEE AP-S Int. Symp. Record.

122. Chen, M.H., and Tsandoulas, G.N. (1973) Bandwidth properties of quadruple-ridged circular and square waveguide radiators, IEEE AP-S Int. Symp. Record, 391-394.

123. Tsandoulas, G.N., and Knittel, G.H. (1973) The analysis and design of dual-polarization square waveguide phased arrays, IEEE Trans. AP-21: 796-808.

124. Hsiao, J.K. (1971) Analysis of interleaved arrays of waveguide elements, IEEE Trans. AP-19:729-735.

125. Boyns, J.E., and Provencher, J.H. (1972) Experimental results of a multi-frequency array antenna, IEEE Trans. AP-20:106-107.

126. Hsiao, J.K. (1972) Computer aided impedance matching of a interleaved waveguide phased array, IEEE Trans. AP-20:505-506.

127. Harper, W.H., et al (1972) NRL Report No. 7369, Naval Research Laboratory.

128. Munson, R.E. (1974) Conformal microstrip antennas and microstrip phased arrays, IEEE Trans. AP-22:74-78.

129. Howell, J.Q. (1975) Microstrip antennas, IEEE Trans. AP-23:90-93.

130. Kaloi, C. (1975) Asymmetrically Fed Electric Microstrip Dipole Antenna, TR-75-03, Naval Missile Center, Point Magee, CA.

131. Derneryd, A. (1976) Linearly polarized microstrip antennas, IEEE Trans. AP-24:846.

132. Microwave Journal, Special Issue (1977) Solid State power, 20(No. 2).

133. Stern, E., and Tsandoulas, G.N. (1975) Ferroscan: Toward continuous-aperture scanning, IEEE Trans. AP-23(No. 1):15-20.

134. Walton, J.D., editor (1970) Radome Engineering Handbook, Georgia Tech.

135. Wait, J.R. (1976) Theories of scattering from wire grid and mesh structures, Proc. of National Conference on Electromagnetic Scattering, University of Illinois.

136. Collin, R.E. (1955) Theory and design of wideband multisection quarter-wave transformers, Proc. IRE 43(No. 2):179-185.

137. Collin, R.E. (1960) Field Theory of Guided Waves, McGraw-Hill, 79-93.

138. Kieburtz, R.B., and Ishimaru, A. (1962) Aperture fields of an array of rectangular apertures, IRE Trans. AP-9:663-671.

139. Chen, C.C. (1971) Diffraction of electromagnetic waves by a conducting screen perforated periodically with circular holes, IEEE Trans. MTT-19 (No. 5):475-481.

140. Pelton, E.L., and Monk, B.A. (1974) A streamlined metallic radome, IEEE Trans. AP-22(No. 6):799-804.

141. Luebbers, R.J. (1976) Analysis of Various Periodic Slot Array Geometries Using Modal Matching, Report AFAL-TR-75-119, Ohio State University.

142. Monk, B.A., et al (1974) Transmission through a two layer array of loaded slots, IEEE Trans. AP-22:804-809.

143. Young, L., Robinson, L., and Hacking, C. (1973) Meanders-line polarizer, IEEE Trans. AP-21:376-378.

144. Lerner, D.S. (1965) A wave polarization converters for circular polarization, IEEE Trans. AP-13:3-7.

145. Mailloux, R.J. (1976) Synthesis of spatial filters with Chebyshev characteristics, IEEE Trans. Antennas and Propagation AP-24(No. 2)174-181.

146. Cohn, S.B. (1955) Optimum design of stepped transmission-line transformers, IRE Trans. MTT MTT-3(No. 2)16-21.

147. Riblet, H.J. (1957) General synthesis of quarter-wave impedance transformers, IRE Trans. MTT MTT-5(No. 1)36-43.

148. Young, L. (1959) Tables for cascaded homogeneous quarter-wave transformers, IRE Trans. MTT MTT-7(No. 2)233-244.

149. Young, L. (1962) Stepped-impedance transformers and filter prototypes, IRE Trans. MTT MTT-10(No. 5):339-359.

150. Mathai, G., Young, L., and Jones, E.M.T. (1964) Microwave Filters, Impedance Matching Networks and Coupling Structures, New York, McGraw-Hill, Chapter 9.

METRIC SYSTEM

BASE UNITS:

Quantity	Unit	SI Symbol	Formula
length	metre	m	...
mass	kilogram	kg	...
time	second	s	...
electric current	ampere	A	...
thermodynamic temperature	kelvin	K	...
amount of substance	mole	mol	...
luminous intensity	candela	cd	...

SUPPLEMENTARY UNITS:

plane angle	radian	rad	...
solid angle	steradian	sr	...

DERIVED UNITS:

Acceleration	metre per second squared	...	m/s
activity (of a radioactive source)	disintegration per second	...	(disintegration)/s
angular acceleration	radian per second squared	...	rad/s
angular velocity	radian per second	...	rad/s
area	square metre	...	m
density	kilogram per cubic metre	...	kg/m
electric capacitance	farad	F	A·s/V
electrical conductance	siemens	S	A/V
electric field strength	volt per metre	...	V/m
electric inductance	henry	H	V·s/A
electric potential difference	volt	V	W/A
electric resistance	ohm		V/A
electromotive force	volt	V	W/A
energy	joule	J	N·m
entropy	joule per kelvin	...	J/K
force	newton	N	kg·m/s
frequency	hertz	Hz	(cycle)/s
illuminance	lux	lx	lm/m
luminance	candela per square metre	...	cd/m
luminous flux	lumen	lm	cd·sr
magnetic field strength	ampere per metre	...	A/m
magnetic flux	weber	Wb	V·s
magnetic flux density	tesla	T	Wb/m
magnetomotive force	ampere	A	...
power	watt	W	J/s
pressure	pascal	Pa	N/m
quantity of electricity	coulomb	C	A·s
quantity of heat	joule	J	N·m
radiant intensity	watt per steradian	...	W/sr
specific heat	joule per kilogram-kelvin	...	J/kg·K
stress	pascal	Pa	N/m
thermal conductivity	watt per metre-kelvin	...	W/m·K
velocity	metre per second	...	m/s
viscosity, dynamic	pascal-second	...	Pa·s
viscosity, kinematic	square metre per second	...	m/s
voltage	volt	V	W/A
volume	cubic metre	...	m
wavenumber	reciprocal metre	...	(wave)/m
work	joule	J	N·m

SI PREFIXES:

Multiplication Factors	Prefix	SI Symbol
$1\,000\,000\,000\,000 = 10^{12}$	tera	T
$1\,000\,000\,000 = 10^{9}$	giga	G
$1\,000\,000 = 10^{6}$	mega	M
$1\,000 = 10^{3}$	kilo	k
$100 = 10^{2}$	hecto*	h
$10 = 10^{1}$	deka*	da
$0.1 = 10^{-1}$	deci*	d
$0.01 = 10^{-2}$	centi*	c
$0.001 = 10^{-3}$	milli	m
$0.000\,001 = 10^{-6}$	micro	μ
$0.000\,000\,001 = 10^{-9}$	nano	n
$0.000\,000\,000\,001 = 10^{-12}$	pico	p
$0.000\,000\,000\,000\,001 = 10^{-15}$	femto	f
$0.000\,000\,000\,000\,000\,001 = 10^{-18}$	atto	a

* To be avoided where possible.

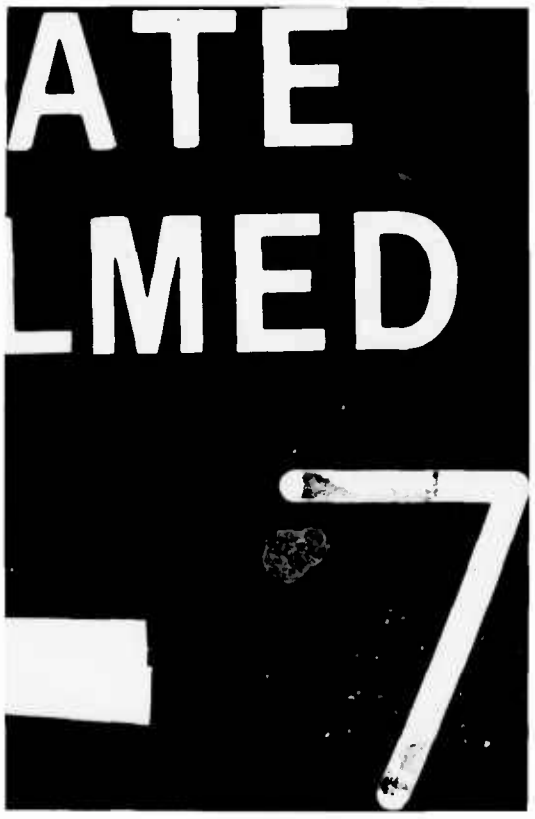
ATE
LMED
7